# Paleohydrological changes over the last 50 ky in the central Gulf of Cadiz: Complex forcing mechanisms mixing multi-scale processes

**PENAUD Aurélie** [(a)] *, **EYNAUD Frédérique** [(b)]

**VOELKER Antje Helga Luise** [(c,d)], **TURON Jean-Louis** [(b)]

*(a) Univ Brest, CNRS, UMR 6538 Domaines Océaniques, IUEM, 29280, Plouzané, France.*

*(b) Univ Bordeaux, CNRS, UMR 5805 EPOC, Allée Geoffroy St Hilaire, 33615, Pessac, France.*

*(c) Divisão de Geologia e Georecursos Marinhos, Instituto Português do Mar e da Atmosfera (IPMA), Rua Alfredo Magalhães Ramalho 6, 1495-006 Lisboa, Portugal*

*(d) CCMAR, Centro de Ciencias do Mar, Universidade do Algarve, Campus de Gambelas, 8005-139 Faro, Portugal*

*Corresponding author.

Tel.: +33-298-498-741; fax: +33-298-498-760.

*E-mail address:* aurelie.penaud@univ-brest.fr

**ABSTRACT**

New dinoflagellate cyst (dinocyst) analyses were carried out at high-resolution in core MD99-2339, retrieved from a contouritic field in the central part of the Gulf of Cadiz, for the Marine Isotope Stage (MIS) 3 interval, allowing to discuss paleohydrological changes over the last 50 ky in the subtropical NE Atlantic Ocean. Some index dinocyst taxa, according to their (paleo) ecological significance, shed light on significant sea-surface changes. Superimposed on the general decreasing pattern of dinocyst export to the seafloor over the last 50 ky, paralleling the general context of decreasing aeolian dust fertilization, a complex variability in dinocyst assemblages was detected at millennial time scale. Enhanced fluvial discharges occurred during Greenland Interstadials (GI) and especially GI 1, 8 and 12, while enhanced upwelling cell dynamics were suggested during the Last Glacial Maximum and Heinrich Stadials. Finally, during the early Holocene, and more specifically during the Sapropel 1 interval (around 7-9 ka BP), we evidenced a strong decrease in dinocyst fluxes, which occurred synchronously to a strong reduction in Mediterranean Outflow Water strength, and that we attributed to an advection of warm and nutrient-poor subtropical North Atlantic Central Waters. Over the last 50 ky, our study thus allows capturing and documenting the fine tuning existing between terrestrial and marine realms in North Atlantic subtropical latitudes, not only in response to the regional climate pattern, but also to monsoonal forcing interfering during precession-driven northern hemisphere insolation maxima. This mechanism, well expressed during the Holocene, is superimposed on the pervasive role of the obliquity as a first major trigger for explaining migration of dinocyst productive centres in the NE Atlantic margin to the subtropical (temperate) latitudes during glacial (interglacial) periods.

*KEYWORDS: Gulf of Cadiz; Dinoflagellate cysts; Dansgaard-Oeschger events; Lingulodinium machaerophorum; Obliquity and precession forcing; Paleoriver discharges; Upwelling.*

## 1. INTRODUCTION

Marginal and semi-enclosed seas, continental shelves and especially upwelling cells or river mouths, are marine regions characterized by high primary productivity conditions. They play an important role as a carbon sink and then significantly contribute to $CO_2$ storage. In this context, the North Atlantic is the major contributor to atmospheric $CO_2$ sequestration (Sabine et al., 2004; Takahashi et al., 2009), especially in high latitudes, even if uncertainties remain on the calculated amount stored by coastal regions (e.g. Flecha et al., 2012). Disregarding abiotic processes, $CO_2$ storage evolution is itself substantially governed by continental and marine primary producers through biological carbon fixing, export and fossilization. The majority of ocean primary production comes from micro-phytoplanktonic organisms (mostly diatoms, coccolithophores and dinoflagellates; Falkowski and Raven, 1997), mainly in coastal upwelling systems as well as in temperate and subpolar regions; these micro-organisms being extremely sensitive to climate changes at seasonal and interannual time scales. In this study, we targeted a major component of the modern phytoplanktonic biomass, the dinoflagellate group. About 15% of living dinoflagellate species form highly resistant resting cysts (dinocysts) after sexual reproduction (Dodge and Harland, 1991; Head, 1996; Dale, 1996) whose modern distribution is tightly coupled to sea-surface physico-chemical characteristics (nutrient availability, temperature, sea-ice cover duration, salinity or light penetration; Rochon et al., 1999; Marret and Zonneveld, 2003; de Vernal et al., 2001, 2005; de Vernal and Marret, 2007; Zonneveld et al., 2013). Dinocysts recorded in marine sediments thus enable to discuss qualitatively as well as quantitatively past surface environments; their preservation being furthermore high in comparison to other fossilisable planktonic groups suffering from dissolution issues of authigenic silica and carbonates (e.g. de Leeuw et al., 2006).

The central Gulf of Cadiz is a place of low present-day marine productivity, with a moderate responsibility for $CO_2$ and $CH_4$ storage (e.g. Huertas et al., 2006, 2009; Flecha et al, 2012).

However, this might not have been the case in the past due to the potential migration of proximal productive centres (e.g. Portugal and Moroccan upwelling centres) at long-term orbital time scales (glacial-interglacial cycles) as well as at millennial sub-orbital ones (i.e. the well-known Greenland Interstadial (GI) / Greenland Stadial (GS) cycles; Dansgaard et al., 1993; Grootes et al., 1993). In fact, it was demonstrated that productivity changes in this region involve complex hydrographical dynamics, including upwelling (Abrantes 1991, 1992), river inputs, also probably additionally forced by Mediterranean-Atlantic exchanges (Rogerson et al., 2012; Ivanovic et al., 2013). Our study aims to explore how these changes may have impacted dinoflagellates, here viewed as an index planktonic group, so as to understand complex patterns and couplings of paleohydrological and paleoproductivity changes over the last 50 ky in the subtropical NE Atlantic. Large environmental shifts which have characterized the studied period are known to be well expressed and preserved in the Gulf of Cadiz sedimentological archives (e.g. Sierro et al., 2005; Voelker et al., 2006, 2015; Toucanne et al., 2007; Peliz et al., 2009; Rogerson et al., 2010, 2012; Bahr et al., 2014, 2015; Hernandez-Molina et al., 2014), thus providing an ideal case study for our purposes. Different configurations of Mediterranean-Atlantic exchanges were also taken into account regarding their potential impacts on MD99-2339 dinocyst surface proxies. For this paper, we focus on the paleohydrographical response of the Gulf of Cadiz during Marine Isotope Stage (MIS) 3 to extend previous studies that extensively documented the last glacial/interglacial transition (e.g. Rogerson et al., 2004; Turon et al., 2003; Penaud et al., 2010). We also consider the Northern Hemisphere paleoclimatological changes within a broader subtropical climate context, including the Mediterranean Basin (Bahr et al., 2015).

## 2. SURFACE AND DEEP HYDROGRAPHY OF THE GULF OF CADIZ

The study area is located on the oriental part of the North Atlantic's subtropical gyre directly adjacent to the Gibraltar Strait (<14km width, <300m depth); the latter channelling water mass exchanges between Atlantic waters at the surface and saltier/denser Mediterranean Outflow Waters (MOW) at depth. This area thus associates the convergence of critical water masses regarding the Atlantic Meridional Overturning Circulation (AMOC) with a semi-permanent upwelling regime, itself connected to the larger dynamic cells off NW Africa.

More specifically, sea-surface waters from the Gulf of Cadiz are influenced by several features which are: the Portuguese and Moroccan coastal currents, a branch of the Azores Current (AzC; Figure 1) flowing eastward at 35°N (Peliz et al., 2009), and the MOW also contributing to the generation of the AzC that feeds the Canary Current (CC; Figure 1) to the South. In the open ocean only, the AzC coincides with the Azores Front (AF), forming a strong hydrographical barrier at the northeastern boundary of the Atlantic subtropical gyre marked both in terms of temperature gradients (about 4°C; Gould, 1985) and vertical structure of the water column (Fasham et al., 1985). This front is locally characterized by intense upwelling cells and thus higher sea-surface productivity (Rudnick, 1996; Alves and de Verdière, 1999; Alves et al., 2002). Nowadays, the AF does not penetrate into the Gulf of Cadiz where the upper 50 m sea-surface waters are generally depleted in nutrients (Navarro and Ruiz, 2006). The Gulf of Cadiz is thus today moderately responsible for $CO_2$ storage (e.g. Huertas et al., 2006, 2009; Flecha et al, 2012), and this oligotrophic regime is mainly due to surface inflow of relatively nutrient-depleted Atlantic water, while nutrient-richer conditions are found at depth as remnant Antarctic Intermediate Waters (Cabeçadas et al., 2002, 2003).

On the northeastern shelf of the Gulf of Cadiz, it has been demonstrated that present-day river discharges (freshwater inputs from large rivers such as the Guadania, Tinto-Odiel and especially the Guadalquivir on the southern Iberian margin), in combination with meteorological conditions

(incident irradiance, strong winds), strongly impact phytoplankton biomass (Huertas et al., 2006). More specifically, turbidity-plume and chlorophyll-concentration dynamics shed light on enhanced primary-productivity conditions related to fluvial discharges occurring during rainy seasons, and especially during negative modes of the North Atlantic Oscillation (NAO) (Caballero et al., 2014). The central Gulf of Cadiz is, conversely, rather subject to fluvial influences from NW Moroccan rivers (especially from the Sebou River and additional northern African small distributaries) for which plumes spread over a large coastal area (Warrick and Fong, 2004). Additionally, the wind pattern is highly significant for sea-surface biological processes within the Gulf of Cadiz (Navarro and Ruiz, 2006): the wind-related mixing phenomenon cumulates with the wind-driven coastal upwelling regime, active mainly from late May / early June to late September / early October in the Portugal-Canary system (e.g. Haynes et al., 1993; Aristegui et al., 2005; Peliz et al., 2005). This seasonal upwelling functioning is itself dependent on seasonal migrations of the Azores High coupled to the Intertropical Convergence Zone dynamics (Hsu and Wallace, 1976). Over the last 30 ky, the evidence of extremely close paleohydrological patterns between the central Gulf of Cadiz and the NW Moroccan margin supported the idea of similar forcing acting on both these subtropical areas of the NE Atlantic margin (Penaud et al., 2011a).

Water masses from our study area are structured as follow: Surface Atlantic Waters, between the surface and 100 m water depth, overlay North Atlantic Central Waters, found between 100 and 700 m. Deep MOW are divided into two main branches centred at around 800 and 1,200 m water depths, and also at 500 m in the continental shelf (Ambar and Howe, 1979; Ambar et al., 2002). North Atlantic Deep Waters are found below 1,500 m (Alvarez et al., 2005).

## 3. MATERIAL AND METHODOLOGY

### *3.1. Marine cores integrated within the study: chrono-stratigraphy*

Core MD99-2339 (35.89°N; 7.53°W; 1170 m water depth; 18.54 m length; Figure 1) was recovered from a contouritic field (Habgood et al., 2003) by the R/V Marion Dufresne during the 1999 International Marine Global Change Studies V (IMAGES V-GINNA) cruise (Labeyrie et al., 2003). It covers the last 45 ky according to its published age model (Voelker et al., 2006) that is based on 20 AMS $^{14}C$ dates and three $\delta^{18}O$ control points tuned to the GISP2 chronology (Grootes and Stuiver, 1997).

In this study, the stratigraphical framework of core MD99-2339 was re-considered for its older part, where radiocarbon dates exhibited large error bars (between 200 years around 900 cm and 1,400 years at 1500 cm; Voelker et al., 2006; Figure 2) and inconsistencies with the regional North Atlantic stratotype NGRIP GICC05 time scale (Svensson et al., 2008; Austin and Hibbert, 2012; Austin et al., 2012; Rasmussen et al., 2014). This revision was furthermore motivated by the comparison of this new dinocyst MIS 3 record to that of core MD95-2043 (Alboran Sea; 36.14 °N; 2.62°W; 1841 m water depth; 36 m length; Penaud et al., 2011b; Figure 1). Such an approach is validated by previous works conducted on the southern Iberian margin where the stratigraphy of paleoclimatological reference sites were constructed using a similar tuning to Greenland ice records (e.g. Shackleton et al., 2000; Bard et al., 2004). This event based stratigraphy (i.e., Austin and Hibbert, 2012), however, prevents establishing any definitive conclusion about latitudinal leads and lags, and evaluating intra-hemispheric propagation velocities of climatic perturbations. To build the revised age-depth model (Figure 2), we chose to keep six radiocarbon dates (Voelker et al., 2006; Figures 2 and 3) younger than 20 ka BP (until around 600-700 cm; mean errors of 60 years) that we calibrated to calendar years with the CALIB 7.1 program using the Marine13 calibration data (Stuiver and Reimer, 1993; Reimer et

al., 2013). Below 700 cm, we tuned the planktonic monospecific $\delta^{18}O$ record (*G. bulloides*) of core MD99-2339 (thirteen pointers; Figures 2 and 3) to the NGRIP ice-core GICC05 chronology, considering synchronous sea-surface warmings in the Gulf of Cadiz with the onsets of GI 3 to 12, respectively (Wolff et al., 2010). As a result, Heinrich Stadial (HS, Barker et al., 2009; Sánchez-Goñi and Harrison, 2010) 5 (HS 5) is dated around 48 ka BP in our revised age model rather than 45-46 ka BP (Voelker et al., 2006; Figure 2). Sedimentation rates show a general decreasing trend from 60-90 cm/ky around 40-45 ka BP to 10-40 cm/ky across the Holocene (Figure 3).

### *3.2 Dinoflagellate cyst analysis*

#### *3.2.1. Laboratory procedure and microscopic observation*

161 samples were analysed for their dinocyst content every 10 cm in average, representing a sample resolution of around 300 years [σ=210]) for the whole MD99-2339 core, using an Olympus BX50 microscope at 400X magnification (75 slides from 0 to 740 cm / 0 to 27 ka BP: Penaud et al., 2011a; 86 slides from 750 to 1844 cm / 27 to 49 ka BP: this study). The preparation technique followed the protocol described by de Vernal et al. (1999) and Rochon et al. (1999), slightly modified at the EPOC laboratory (Castera and Turon, http://www.epoc.u-bordeaux.fr/index.php?lang=fr&page=eq_paleo_pollens), including chemical treatments (cold HCl: 10, 25 and 50% and cold HF: 45 and 70%) and sieving through single-use 10 µm nylon mesh screens. The final residue was then mounted between slide and coverslip with glycerine jelly coloured with fushin.

For each analysed sample, a minimum of 300 dinocyst specimens were systematically identified following the taxonomy in Fensome and Williams (2004) and Fensome et al. (2008). High occurrences of the species *Lingulodinium machaerophorum* (nearly monospecific in some cases but typical for the area today) forced us to additionally count 100 dinocysts outside this species for each palynological slide to obtain statistically robust dinocyst results (Fatela and Taborda,

2002). Dinocysts can be expressed in percentages and also in concentrations (number of specimens/$cm^3$ of dry sediments), that are calculated through the marker grain method (Stockmarr, 1971; de Vernal et al., 1999; Mertens et al., 2009). This consists in adding aliquot volumes of *Lycopodium* spores before the palynological treatment in each sample; these exotic spores being counted in parallel with fossil palynomorphs. One can argue that there might be a relationship between concentrations and granulometry (increasing / decreasing concentrations *versus* increasing clays-fine silts / coarser silts-fine sands; Wall et al., 1977), especially in a contouritic environment. However, it is important to note that only fine silts have been sampled for palynological analysis. Furthermore, given that cyst concentrations are the combined results of sedimentation rates, grain-size and productivity, we also calculated flux rates (number of cysts/$cm^2$/ky). We do not have enough time marker points to calculate flux rates for every single short event separately but, at least on a multi-millennial time scale, dinocyst fluxes may provide a better insight on dinocyst export to the seafloor, and perhaps also indirectly on dinoflagellate productivity in surface waters.

*3.2.2. Dinocyst indexes and Statistical treatments of dinocyst results*

***Warm / Cold ratio***

The present-day ecology of many of the recovered species is well known from their surface sediment distribution in the North Atlantic (e.g. Turon, 1984; Rochon et al., 1999). Furthermore, latitudinal (SST changes) and inshore-offshore (eutrophic-oligotrophic conditions) gradients are mainly responsible for dinocyst distribution in modern sediments (Marret and Zonneveld, 2003; Zonneveld et al., 2013). A qualitative thermic index “Warm/Cold” (W/C), which has previously been used to qualitatively address SST variations (Turon and Londeix, 1988; Versteegh, 1994; Combourieu-Nebout et al., 1999; Eynaud et al., 2016), was calculated for MD99-2339 core (cf. Table 1).

***Heterotrophic / Autotrophic ratio***

Most dinoflagellate species are mixotrophic, and strict autotrophic (phototrophic organisms) are rare. However, previous investigations discussed heterotrophic cysts, i.e. derived from dinoflagellates with a strict heterotrophic strategy of nutrition, as being indirectly related to food resources, and especially diatoms, as it has commonly been shown in upwelling areas (Wall et al., 1977; Lewis et al., 1990; Marret, 1994; Biebow, 1996; Zonneveld et al., 1997a, 2001; Targarona et al., 1999; Bouimetarhan et al., 2009; Penaud et al., 2011a). This is especially true for *Protoperidinium* species, including *Brigantedinium* and *Selenopemphix* species, thus indirectly signing periods of higher surface water productivity. In the following sections of the paper, we will refer these taxa as "heterotrophics"; "coastal heterotrophics" being more specifically used for *Selenopemphix* species (*S. quanta* and *S. nephroides*; Table 1). Also a ratio "Heterotrophics / Autotrophics" (H/A) can be addressed that simply takes into account "strict" heterotrophic occurrences *versus* the other dinocyst taxa identified in fossil assemblages.

***Diversity statistics***

Quantifying taxonomical diversity in study samples was carried out through a variety of statistical analyses using the "Past version 1.75b" software (Hammer et al., 2001); most of these indexes being explained in Harper (1999). Here, we calculated the number of taxa per sample (S), the dominance (D) that ranges from 0 (all taxa are equally present) to 1 (one taxon dominates the community completely), and Margalef's richness index: $(S - 1)/ \ln(n)$, where n is the number of individuals counted in each sample.

***Quantitative estimates of past sea-surface parameters***

We used the Modern Analogue Technique (MAT) based on the statistical distance between fossil (paleoceanographic record) and current (modern database) assemblages (de Vernal et al., 2001; 2005; Guiot and de Vernal; 2007). The dinocyst transfer function used (Radi and de Vernal, 2008) is derived from a modern database comprising 67 dinocyst species and 1,492 stations from the North Atlantic, Arctic and North Pacific oceans and their adjacent seas, and is run under the "R version 2.7.0" software (R Development Core Team, 2008; http://www.r-project.org/). The calculation of past hydrological parameters relies on a weighted average of the values obtained for a maximum of five best modern analogues for fossil assemblages; the maximum weight being given for the closest analogue (i.e. minimal statistical distance, or "Dmin). If "Dmin" reaches a maximal threshold value, the "R" software will consider no analogue, leading then occasionally to non analogue configurations. Here, we discuss Winter/Summer SST with prediction errors of ±1.2°C/±1.6°C, respectively, Winter/Summer SSS, with prediction errors of ±2.1°C/±2.3°C, respectively, as well as primary productivity reconstructions with prediction error of 57 $gC.m^{-2}$.

## 4. MAIN DINOCYST RESULTS ACROSS THE LAST 50 KY IN THE GULF OF CADIZ

### *4.1. Dinocyst diversity, concentrations, and fluxes*

A total of 40 taxa was identified, with an average diversity of 20 main species. Considering the whole dinocyst assemblage, increased total diversity (Figure 4c) generally appears anti-correlated to decreased dominance (Figure 4d); this index being essentially explained by *Lingulodinium machaerophorum* percentages through time (Figure 4e) that oscillate between 30 and 90%. *L. machaerophorum* is commonly considered as a typical index species for stratified waters (Table 1; Zaragosi et al., 2001; Penaud et al., 2009; Holzwarth et al., 2010), thus probably indicating enhanced fluvial inflows. Since core MD99-2339 is located in the major flow path of the lower limb of the MOW, and in a position also corresponding to the major limb of the MOW during the LGM (Rogerson et al., 2011), one can speculate if the paleoceanographical record has been disturbed by MOW plume hydrodynamics or advection by sedimentological processes (i.e. downslope transport). Large increase of monospecific assemblages (when dominance is close to 1) will generally tend to reduce diversity and conversely (dominance close to 0 reflecting an equidistribution of different species when the diversity is maximum). Based on the obvious anti-correlation depicted in Figure 4 (diversity *versus* dominance), we argue for an autochthonous assemblage where species, and especially *L. machaerophorum*, reflect an *in situ* signal linked to changing sea-surface conditions.

Total dinocyst concentrations are generally low (less than 30,000 cysts/$cm^3$), with the exception of two large maxima, centred on GI 8 and GI 12, showing higher values (between 100,000 and 400,000 cysts/$cm^3$) (Figure 4f). A general trend of decreasing concentrations is then observed throughout the record with lower values observed during the early to mid-Holocene (between 1,000 and 10,000 cysts/$cm^3$) and especially at the very start of the Holocene (1,500 cysts/$cm^3$; at 150-200 cm), following the cold interval of the Younger Dryas (YD) (Figure 4f). Also, minimum concentration values recorded during MIS 3 are comparable to maximum values recorded during

278 the following MIS 2 and MIS 1. The general trend described above closely matches the one of
279 the sedimentation rates (Figure 4h) and thus also accounts for extremely high dinocyst fluxes to
280 the seafloor during MIS 3 (Figure 4j), compared to the last deglaciation and the Holocene. Total
281 dinocyst concentrations are mainly explained by *L. machaerophorum* alone (Figure 4h), showing
282 the crucial role of this species regarding dinocyst export to the seafloor from the last glacial to
283 present in this subtropical NE Atlantic area. While heterotrophics represent a minor component
284 of total dinocyst concentrations all along the core (Figure 4g), it is interesting to note that both
285 heterotrophic and *L. machaerophorum* concentrations / fluxes reveal the same decreasing trend
286 along the record (Figure 4j). Previous studies have revealed contrasted patterns between brown
287 heterotrophic and *L. machaerophorum* cysts. Their apparent conflict is discussed at long time
288 scales on the southern Iberian margin area in Eynaud et al. (2000, 2016).
289
290 ***4.2. Dinocyst species reflecting qualitatively main paleohydrological changes***
291 Present-day ecologies of major species found in MD99-2339 assemblages are listed in Table 1
292 with their major past occurrences in the fossil record. The detailed examination of the qualitative
293 thermic index "Warm/Cold" (W/C) (Table 1; Figure 5; cf. subchapter 3.2.2 of this paper),
294 compared with the planktonic $\delta^{18}O$ curve (*G. bulloides*) of core MD99-2339 (Voelker et al.,
295 2006), shows that millennial-scale climate variability related to the GS / GI cycles is clearly
296 captured by our fossil record then confirming the robustness of reconstructed surface
297 environments through dinocyst assemblages in the central Gulf of Cadiz.
298 Specific percentages, calculated relatively to the total dinocyst assemblages but also *versus* a total
299 that excludes *L. machaerophorum*, reveal that trends with or without *L. machaerophorum* are
300 similar (Figure 5). Peak occurrences are, however, better expressed when *L. machaerophorum* is
301 omitted from the main palynological sum. Figure 5 furthermore includes the published data from
302 core MD04-2805 CQ (Figure 1) over the last 28 ky (Penaud et al., 2010; dotted lines in Figure 5).

Obvious correlation between surface conditions recorded off the NW Moroccan coast (Marret and Turon, 1994; Penaud et al., 2010) and in the central part of the Gulf of Cadiz may be due to same dynamics governing paleohydrological changes in this sector (Penaud et al., 2011a). Considering more specifically hetrotrophics, these are never dominant among studied assemblages (Figure 5). Heterotrophics are well known to be sensitive to oxic conditions (e.g. Combourieu-Nebout et al., 1998; Zonneveld et al., 1997b; Kodrans-Nsiah et al., 2008), and the fact that *Brigantedinium* percentages increased during GS (i.e. periods with relatively well-oxygenated bottom waters related to MOW dynamics) may argue for a negligible effect of oxidation processes on species-selective degradation after cyst deposition in our study site. Significant occurrences of some selected species (Table 1; Penaud et al., 2011a), and especially coastal heterotrophics (*S. quanta* and *S. nephroides*; Figure 5), will then indirectly reflect varying regimes of mesotrophic-oligotrophic conditions in the Gulf of Cadiz over the last 50 ky.

## 5. UNDERLYING MECHANISMS BEHIND DINOCYST CHANGES AT ORBITAL AND SUB-ORBITAL TIME SCALES IN THE GULF OF CADIZ

Portuguese-Moroccan upwelling dynamics are of particular interest since planktonic populations are directly linked there to frontal areas and upwelled nutrient-enriched waters. At the Quaternary time scale, biodiversity increases have previously been observed during glacial periods, as a probable consequence of an enhanced functioning of upwelling cells (Abrantes, 1988, 1991; Targarona et al., 1999; Penaud et al., 2011a) and strong biodiversity modifications have been related to abrupt climate changes such as cold GS and especially HS (Lebreiro et al., 1997; Eynaud et al., 2000; Voelker et al., 2006; Penaud et al., 2011a, b) with a total re-structuration of the water column. Understanding mechanisms underlying the complex pattern of paleoproductivity changes at orbital as well as millennial time scales thus includes considering a wide range of external and internal forcing, i.e. varying conditions in terms of sea level, insolation, wind-stress, water-mass exchanges at the Gibraltar Strait, iceberg or fluvial discharges, and frontal upwelling cells; all of these being more or less inter-connected at different time scales.

### *5.1. Glacial fertilisation control on marine surface productivity*

Annual productivity quantifications calculated from dinocyst transfer function (Figure 6), the qualitative ratio H/A, as well as dinocyst fluxes (total and heterotrophics), evidence higher productivities during the Late Glacial compared to the Holocene, with a sharp transition especially noted at 15 ka BP (Figure 6). Similar decreasing paleo-productivity at the end of the last glacial period (Voelker et al., 2009) was also previously discussed in the Gulf of Cadiz in a nearby core (GeoB 9064; 35°24.91′N, 06°50.72′W, 702 m water depth) based on planktonic foraminifera-derived productivity quantifications (Wienberg et al., 2010). Glacial productivity rise is commonly attributed to a fertilisation effect caused by increasing aeolian dust supply to the

ocean under stronger glacial winds (Moreno et al., 2002; Bout-Roumazeilles et al., 2007; Wienberg et al., 2010), combined with higher Mediterranean continental aridity (Combourieu-Nebout et al., 2002; Sánchez-Goñi et al., 2002; Bar-Matthews et al., 2003; Fletcher and Sánchez-Goñi, 2008). Also, during MIS 2, glacial productivity reconstructed in the Gulf of Cadiz through dinocyst assemblages are the highest (around 500 gC/m² compared to present-day values of about 90 gC/m²; Figure 6). It was suggested to be regionally due to upwelled nutrient-enriched waters linked to the occurrence of a comparable hydrographic barrier to the modern Azores Front (Rogerson et al., 2004, 2010; Voelker et al., 2009). This is also suggested in our record with enhanced *Brigantedinium* (Figure 7) and total hetrotrophic percentages (H/A; Figure 6) between 26 and 15 ka BP (Penaud et al., 2011a).

### *5.2. Orbital control on paleo-river discharges and nutrient availability*

Furthermore, when considering *L. machaerophorum* percentages *versus* orbital parameters, a very close relationship to the obliquity curve becomes obvious (Figure 7). Assuming this species as a strong fluvial-sensitive cyst (Table 1), we may suggest enhanced precipitation in the southern borderlands of the Mediterranean Basin with obliquity maxima, the latter accounting for increasing northern summer insolation. Furthermore, generally higher percentages of *L. machaerophorum* recorded between 50 and 35 ka BP coincide with extremely high total dinocyst concentrations (fluxes), while generally higher percentages of *L. machaerophorum* recorded from 15 ka BP onwards coincide with extremely low total dinocyst concentrations (fluxes) (Figure 7). The Mediterranean Basin being subject to interference of northern and tropical latitudes, both obliquity and precession signals may be considered. They indeed represent major influences for the East African and West Indian summer monsoon systems (Tuenter et al., 2003) and can be evidenced, for instance, in Mediterranean paleorecords (Lourens et al., 1996, 2001). Furthermore, Tuenter et al. (2003) discussed the fact that the combination “obliquity maxima - precession

366 minima" (cf. MIS 1 in Figure 7) would have a weaker effect on the African monsoon, compared
367 to the combination "obliquity maxima - precession maxima" (cf. MIS 3 in Figure 7). This would
368 be consistent, during MIS 1, with our recorded enhanced stratification related to lower
369 productivities (Figure 6), especially between 10 and 6 ka BP, and our recorded enhanced
370 stratification during periods of higher productivities across the last glacial (Figure 6).
371 Also, interestingly, similar high Gulf of Cadiz dinocyst concentrations (fluxes) and *L.*
372 *machaerophorum* percentages are recorded in the northern Bay of Biscay during the mid-
373 Holocene (Naughton et al., 2007; Ganne A. PhD , Pers. Comm.). We can assume that high
374 nutrient availability in the Gulf of Cadiz during the last glacial may has been similarly high to
375 modern nutrient availability in the northern latitudes of the temperate NE Atlantic (Bay of
376 Biscay). This northward migration of paleo-productive centres is also similar to the migration of
377 cold-water corals, from the Gulf of Cadiz during the last glacial period to the Irish-Norwegian
378 margins at present (Freiwald et al., 2004; Dorschel et al., 2005; Rüggeberg et al., 2007; Eisele et
379 al., 2008; Frank et al., 2005, 2009; de Haas et al., 2009; Wienberg et al., 2009, 2010). We then
380 suggest maxima in dinocyst, and perhaps phytoplanktonic organisms in general, export during
381 glacial obliquity maxima in subtropical latitudes, when ice-sheets were still well developed in the
382 Northern Hemisphere, while interglacial obliquity maxima would preferentially stimulate
383 phytoplanktonic growth in northern latitudes of the North Atlantic. Also, climatic changes
384 affecting the regional freshwater inputs also may contribute to explain those similarities between
385 the last glacial period in the Gulf of Cadiz and the mid-Holocene in the Bay of Biscay (e.g. Sierro
386 et al., 2000; Mikolajewicz, 2011; Bahr et al., 2015; Lofi et al., 2016). Marine surface productivity
387 has been tentatively modelled for the Indian Ocean with simulations coupling a biogeochemical
388 component for primary production, from 80 ka BP climate conditions to the preindustrial state
389 (Le Mézo et al., EGU2015, unpublished data). It evidences the crucial role of obliquity, i.e.
390 glacial-interglacial conditions responsible for changing oceanic circulation, as a main driver for

phytoplanktonic productivities (Hardy et al., 2016).

### *5.3. MIS 3 and the atypical pattern of Greenland Interstadials GI 8 and GI 12*

#### *5.3.1. General overview of MIS 3 pattern on either side of the Strait of Gibraltar*

MIS 3 corresponds to a general stronger velocity of denser MOW export (grain-size analysis; Figure 7). Over this period, dinocyst signals from both sides of the Strait of Gibraltar, i.e. signals recorded from the Gulf of Cadiz (this study) and the Alboran Sea (MD95-2043 core; Penaud et al., 2011b; Figure 1), have been compared so as to qualify Mediterranean-Atlantic surface exchanges at times when MOW experienced strongest/weakest bottom current velocities (Figure 8).

A first look on dinocyst concentrations for selected individual species (Figure 8d,e,f) reveals extremely close patterns from either side of the Strait of Gibraltar, however, with different magnitude of values, especially when considering *L. machaerophorum* concentrations that are 10 to 100 times higher in the Gulf of Cadiz compared to the Alboran Sea (Figure 8d). Total dinocyst concentrations are also characterized by similar temporal fluctuations but different reconstructed values; these marked value differences being only explained by *L. machaerophorum* concentrations since other "autotrophic" species show generally comparable orders of concentrations (Figure 8g).

It is interesting to note that even if individual species concentrations follow obvious identical oscillations, they are not as clear when considering their relative abundances (Figure 8k, l, m). *L. machaerophorum* percentages generally dominate whole cyst assemblages all over MIS 3 in the Gulf of Cadiz, such as today (Rochon et al., 1999; Marret and Zonneveld, 2003; Zonneveld et al., 2013; Table 1; Figure 8k). In the Alboran Sea, *N. labyrinthus* (cool-temperate, outer neritic) percentages mirror *L. machaerophorum* (temperate, inner-neritic) ones in the Gulf of Cadiz (Figure 8l); this species hardly making up 5% of the present-day assemblage in the area. Contrary

to the Gulf of Cadiz, no important river discharges are noticeable today in the Alboran Sea and the continental shelf is narrower. Primary productivity in the Alboran Sea mainly results today from the inflow of Atlantic waters through the Strait of Gibraltar, while marshes and riverine influence in coastal zones from the Gulf of Cadiz is particularly high (Macías et al., 2014). This could explain the predominance of *L. machaerophorum* in MD99-2339 core while *N. labyrinthus* will preferentially characterize MD95-2043 one. When these two species are summed, their percentages show obvious similar patterns both in terms of values and timing of the different recorded peaks (Figure 8n). Combined "*N. labyrinthus* - *L. machaerophorum*" percentages are not clearly related to GS or GI climate conditions, however, features can be distinguished: i) maximal values are recorded at the end of GI 8 and 12, but very low values at the start of these specific interstadials, ii) they never occur during HS with significant percentages, and iii) they often characterize GS climate conditions with increasing relative abundances (Figure 8n).

*5.3.2. Greenland Stadial (GS) and especially Heinrich Stadial (HS)*

During GS, and especially HS, dinocyst seasonal SST reconstructions from the Gulf of Cadiz evidence a 2 to 5°C cooling, as a consequence of the southward shift of the Polar Front (e.g. Eynaud et al., 2009). This is especially true for winter SST (Figure 6); dry and cold winter conditions being also previously recorded in these latitudes (Sánchez-Goñi et al., 2002; Combourieu-Nebout et al., 2002; Moreno et al., 2002, 2005; Bout-Roumazeilles et al., 2007). *B. tepikiense* combined with the polar foraminifera *N. pachyderma* s. attest, respectively, to enhanced seasonality (large offset between summer and winter temperatures as confirmed by dinocyst transfer function; Figure 6) and important coolings in the interval 25-50 ka BP (Figure 6). "*N. pachyderma* s. - *B. tepikiense"* thus evidence in both the Gulf of Cadiz and the Alboran Sea the influx of subpolar water masses into these subtropical northeastern Atlantic latitudes (Bard et al., 2000; Sánchez-Goñi et al., 2000; Pailler and Bard, 2002; Turon et al., 2003; de

441 Abreu et al., 2003; Vautravers and Shackleton, 2006; Eynaud et al., 2000, 2009; Salgueiro et al.,
442 2010, 2014; Patton et al., 2011; Penaud et al., 2011a, b), also accounting for direct and strong
443 surface connections responsible for similar planktonic species occurrences at both sides of the
444 Strait (Figure 8). During HS, this occurs in a context when bottom MOW experienced
445 intermediate (and not the strongest) velocities because of the strong advection of less saline
446 waters at the surface in the Western Mediterranean Basin (Cacho et al., 2000; Sierro et al., 2005;
447 Voelker et al., 2006; Frigola et al., 2008).
448 In the Gulf of Cadiz, during HS, increased annual productivity reconstructions (Figure 6)
449 together with increased heterotrophics (especially *Brigantedinium* spp.; Figure 7), suggest
450 primary productivity increases related to frontal system reorganizations within the Gulf of Cadiz
451 (Rogerson et al., 2004, 2010; Voelker et al., 2009). This front was also discussed over the last 28
452 ky BP by the strong decreasing gradient of *N. pachyderma* s. percentages obvious during HS
453 across a small N-S transect between southern Portugal and the sector Cadiz-Morocco (Penaud et
454 al., 2011a). This configuration is similar to the one previously discussed for the LGM interval
455 that recorded the highest productivities and *Brigantedinium* percentages in our Gulf of Cadiz
456 fossil record (Figures 6 and 7). Except for HS, other GS are not systematically marked by such
457 features. Also, it is interesting to note that productivity drops were noted during GS in the same
458 core with planktonic foraminiferal Cd/Ca values, thus suggesting low nutrient availability at that
459 time (Patton et al., 2011). Our frontal upwelling conditions explaining higher productivities
460 would thus be especially valid for HS climate extrema in the Gulf of Cadiz. In the northern North
461 Atlantic, biomass decline has conversely been linked to abrupt climate changes (Schmittner,
462 2005; Mariotti et al., 2012) during AMOC disruption linked with massive iceberg calving (e.g.
463 McManus et al., 2004; Gherardi et al., 2005).
464
465 *5.3.3. Greenland Interstadial (GI) and especially GI 8 and GI 12: typical bipartite structure*

In the Gulf of Cadiz, warmer surface conditions are generally recorded during GIs, as suggested from the W/C ratio (Figure 5) as well as seasonal SST reconstructions with values close to modern ones (Figure 6). Synchronous occurrences of the thermophilic species *S. mirabilis* on both sides of the Gibraltar Strait (Figure 8c) also indicate general warmer surface conditions at a time when bottom MOW velocity was reduced.

However, GI 12 and GI 8, immediately following HS 5 and HS 4, respectively, are characterized by very peculiar and unique features when compared to other GIs in the core. These two intervals show periods characterized by the longest and strongest expansions of mixed oak forest over MIS 3 (Alboran Sea; Fletcher and Sánchez-Goñi, 2008; Figure 7) and, from a unique hydrological point of view, they can be described according to a bipartite structure in the Gulf of Cadiz (cf. "a" and "b"; Figures 7 and 8), also previously described for the Alboran Sea (Penaud et al., 2011b; cf. Figure 8). While the first part ("a") is characterized by increasing coastal heterotrophics (Figure 8o) and thermophilic species (Figure 8c), paralleling higher polar air temperatures (Figure 8j); the second part ("b") is characterized by the highest total dinocyst concentrations (Figure 8h) and *L. machaerophorum* percentages (Figure 8k) ever recorded over the last 50 ky. This second part is also characterized by a strong *S. mirabilis* drop (Figure 8c), and the lowest winter SST (10°C colder than today; Figure 6) and SSS (around 30 reconstructed at that time; Figure 6). We therefore suggest a major atmospheric reorganization occurring at 37 ka BP within GI 8, and at 45.5 ka BP within GI 12, also detected in NGRIP with decreasing polar temperatures all along these long interstadials (Figure 8j). Within both second phases ("b", Figure 8), synchronous high percentages of *L. machaerophorum* recorded in the subtropical NE Atlantic (quasi monospecific in the Gulf of Cadiz) and in the western Mediterranean basin suggest extremely high fluvial discharges and well-stratified conditions. We therefore suggest an extreme southward shift of the winter westerlies belt, more pronounced during each part "b" than during each part "a", that would also be responsible for huge advection of freshwater, especially during

491 the winter season, and therefore reduced SST and SSS. This questions the feedbacks inherent to
492 the atmospheric/oceanic reorganisations. Even if the precise mechanism underlying this shift is
493 still questioned and would deserve model simulations, our results argue for a fast response of the
494 ocean in this millennial / infra-millennial time scale context of rapid climate change.
495
496 ***5.4. Dinocyst specific pattern across MIS 1***
497 Interestingly, during MIS 1, decreased dinocyst fluxes and increased *Impagidinium* percentages
498 (Figure 7) seem to be related to the humidity pattern as recorded in Western (Fletcher and
499 Sánchez-Goñi, 2008; Figure 7) and Eastern (Bar-Matthews et al., 2000, 2003; Figure 7)
500 Mediterranean records. During the first half of the Bölling-Alleröd (BA), *Impagidinium* species
501 (especially *I. aculeatum*; Figure 5) strongly expand (Figure 7), arguing for the establishment of
502 full oceanic and warm conditions, that may suggest oligotrophic conditions in this area (cf.
503 dinocyst transfer function; Figure 6) progressively replacing glacial eutrophic to mesotrophic
504 ones (Behrenfeld et al., 2005; Wienberg et al., 2010). This shift is synchronous to widespread
505 rainfall over the entire Mediterranean Sea (Toucanne et al., 2015). Increased vegetation cover at
506 that time (Fletcher and Sánchez-Goñi, 2008; Figure 7) and thus decreased river runoff onland
507 may have also induced decreased nutrient supplies to the ocean. It is interesting to note that, in
508 North Atlantic subtropical latitudes, each onset of warm conditions during climatic optima (i.e.
509 MIS 1, MIS 5, MIS 11, and MIS 19) was associated with the expansion of *Impagidinium* species
510 (Eynaud et al., 2016). This group thus marked post-glacial conditions instead of hypsithermal
511 ones when a competition with other thermophilous taxa such as *S. mirabilis* is observed (Turon
512 and Londeix, 1988; Londeix et al., 2007; Eynaud et al., 2000, 2016; Penaud et al., 2008).
513 Noteworthy, and similar to GI 12 and GI 8, the BA is not homogeneous and is marked by a
514 bipartite structure (cf. phases “a” and “b” in Figure 7). The final BA (“b”) is indeed marked by a
515 drastic drop of *Impagidinium* spp., a strong increase of *L. machaerophorum* percentages and high

values of total dinocyst concentrations (Figure 7). This may suggest slightly more productive conditions (cf. Figure 6) that followed mean general Mediterranean aridity increases starting as soon as 14 ka BP and continuing during the following cold event of the YD (Figures 6 and 7).

At the onset of the Holocene, during the 9.5 - 6.5 ka BP interval, the proportion of clay cohesive sediments (cf. grain-size < 63 µm; Figure 7) observed in core MD99-2339 is the largest of the record, then suggesting a strong reduction of MOW flow strength (Voelker et al., 2006), as also evidenced in Western Mediterranean Sea contourites from the Corsica through (Toucanne et al., 2012). This early Holocene interval is coeval with enhanced summer precipitation over the northern borderlands of the Eastern Mediterranean (i.e. North African summer monsoon forcing; Rossignol-Strick, 1983; Rohling and Hilgen, 1991; Bar-Matthews et al., 2000, 2003; Figure 7) and thus increasing summer / autumn fluvial discharges mainly from the Nile (deMenocal et al., 2000; Gasse, 2000). This leads, in the Eastern Mediterranean Sea, to important water column stratification, a cessation of the deep convection, an anoxic phase of bottom waters, high surface productivity, and thus to the organic-rich sapropel 1 formation (e.g. Kallel et al., 1997; Mercone et al., 2000). Also, the Western Mediterranean Basin was subject to enhanced rainfalls (Aritzegui et al., 2000; Zanchetta et al., 2007; Magny et al., 2013), and this has been recently connected to seasonal Mediterranean autumn / winter rainfalls sustaining high fluxes of nutrients and organic matter to the seafloor (Toucanne et al., 2015). Conversely, in our study, the period between 9.5 and 6.5 ka BP is characterized by low quantified productivities (Figure 6), the lowest dinocyst fluxes (Figure 6) and by the highest percentages of *Impagidinium* spp. ever recorded over the last 50 ky BP (Figure 7). Full-oceanic oligotrophic conditions have prevailed in the central Gulf of Cadiz, and this can be attributed to significantly lower amounts of Saharan dust inputs at that time (Wienberg et al., 2010) in a context when Mediterranean forest strongly expanded (Fletcher and Sánchez-Goñi, 2008; Figure 7) preventing dust re-mobilization and run-off. Furthermore, at the time of sapropel 1 formation (Toucanne et al., 2015), a displacement of the autumn / winter

storm track along the northern Mediterranean borderlands (i.e. atmospheric configuration extremely close to a persistence of negative NAO conditions) could have been favourable to a southward winter displacement of the Azores High reinforcing the Azores Current influence towards the Gulf of Cadiz, and therefore also probably the advection of nutrient-poor subtropical North Atlantic Central Water during winter. This would also be consistent with the occurrence of thermophilous *Impagidinium* species, mainly encountered today in fully marine tropical environments (Bouimetarhan et al., 2009). Also, in the Gulf of Cadiz, the Levantine Intermediate Water (LIW) directly contributes to the upper MOW export during interglacials, while a downslope shift of the denser MOW plume is noted during glacials / lowstands (Voelker et al., 2006; Toucanne et al., 2012; Kaboth et al., 2015). We can then hypothesize that, during the Holocene, the cessation of LIW formation in the Eastern Mediterranean Basin may have impacted the remobilization of sediments / nutrients through the lack of mixing at the subsurface between surface and deep currents across the Strait of Gibraltar (Gomez et al., 2000), also additionally contributing to the decreased dinocyst fluxes recorded in the central Gulf of Cadiz (Figure 7).

## 6. CONCLUSION

Marine regions characterized by high primary productivity conditions play an important role as a carbon sink and thus significantly contribute to $CO_2$ storage, and subtropical latitudes deserve a crucial role in the carbon pump at a global scale. Here, new palynological investigations carried out in the central part of the Gulf of Cadiz over MIS 3 (25 - 50 ka BP) enable to consider dinocyst population shifts over the last 50 ky in the subtropical northeastern Atlantic Ocean. This study provides important evidences of migrating paleoproductivity centres from the last glacial period to the Holocene, and can be therefore also of crucial importance for our understanding of

long-term and abrupt climate changes in primary productivity regimes and organic matter export to the seafloor.

We especially focus on the dinocyst species *L. machaerophorum* that we interpret as a powerful tool to discuss surface hydrological changes through time in the northeastern Atlantic, and especially water column stratification under varying regimes of paleo-precipitations, primarily forced by obliquity maxima at orbital time scales. Dinocyst fluxes, and perhaps also dinoflagellate productive conditions, in the Gulf of Cadiz were the highest during the last glacial (especially between GI8 and GI12), and a clear imprint of millennial-scale abrupt climate changes was detected on paleohydrological changes all over the investigated period. During the Holocene, precessional forcing is also suggested through the probable impact of sapropel 1 formation in the Eastern Mediterranean on decreasing dinocyst fluxes and perhaps also on dinoflagellate productivity in the Gulf of Cadiz.

## 7. ACKNOWLEDGMENTS

Thanks to the French polar institute IPEV (*Institut Paul Emile Victor*), the captain and the crew of the Marion Dufresne and the scientific team of the 1995 IMAGES cruise. We wish to thank M. Castera, M. Georget and O. Ther for invaluable technical assistance at the laboratory. This study was supported by the French CNRS and contributes to the 2013 INSU project : « ICE-BIO-RAM : Impact des Changements Environnementaux sur la BIOdiversité marine lors des Réchauffements Abrupts du cliMat » (http://www.insu.cnrs.fr/files/ao_2013_-_eynaud_validee.pdf). This work was supported by the «Laboratoire d'Excellence» LabexMER (ANR-10-LABX-19) and co-funded by a grant from the French government under the program «Investissements d'Avenir». AV acknowledges her Investigador FCT (IF) Development Grant.

## 8. REFERENCES


Abrantes, F., 1988. Diatom assemblages as upwelling indicators in surface sediments off Portugal. Marine Geology 85, 15-39.

Abrantes, F., 1991. Increased upwelling off Portugal during the last glaciation: diatom evidence. Mar. Micropaleontol. 17, 285-310.

Abrantes, F., 1992. Paleoproductivity oscillations during the last 130 ka along the Portuguese and NW African margins, In: Summerhayes, C.P., Prell, W.L., Emeis, K.C. (Eds.), Upwelling Systems: Evolution Since the Early Miocene. The Geological Society, London, pp. 499-510.

Alvarez, M., Pérez, F.F. Shoosmith, D.R. Bryden. H.L. 2005. The unaccounted role of Mediterranean water in the draw–down of anthropogenic carbon. J. Geophys. Res. 110, C09S03, doi: 10.1029/2004JC002633.

Alves, M., de Verdière, A.C., 1999. Instability dynamics of a subtropical jet and applications to the Azores Front current system: Eddy driven mean flow, Journal of Physical Oceanography 29, 837-864.

Alves, M., Gaillard, F., Sparrow, M., Knoll, M., Giraud, S., 2002. Circulation patterns and transport of the Azores Front-current system. Deep-Sea Research II 49, 3 983-4 002.

Ambar, I., Howe, M. R., 1979. Observations of the Mediterranean outflow - I: Mixing in the Mediterranean outflow. Deep-Sea Res. 26, 535-554.

Ambar, I., Serra, N., Brogueira, M.J., Cabecadas, G., Abrantes, F., Freitas, P., Goncalves, C., Gonzalez, N., 2002. Physical, chemical and sedimentological aspects of the Mediterranean outflow off Iberia. Deep-Sea Research II 49, 4163-4177.

Aristegui, J., Alvarez-Salgado, X.A., Barton, E.D., Figueiras, F.G., Hernandez-Leon, S., Roy, C., Santos, A.M.P., 2005. Chapter 23: oceanography and fisheries of the Canary current/Iberian region of the eastern North Atlantic (18a,E). In: Brink K.H. (ed.), Robinson A.R. (ed.) The sea : the global coastal ocean : interdisciplinary regional studies and syntheses. Harvard: Harvard University Press, 877-931.

Ariztegui, D., Asioli, A., Lowe, J., Oldfield, F., 2000. Palaeoclimatic reconstructions and formation of sapropel S1: Inferences from Late Quaternary lacustrine and marine sequences in the Central Mediterranean region. Paleoceanography, Paleoclimatology, Palaeoecology 158, 215-240.

Austin, W.E.N., Hibbert, F.D., 2012. Tracing time in the ocean: A brief review of chronological constraints (60–8 kyr) on North Atlantic marine event-based stratigraphies, Quat. Sci. Rev., 36, 28-37.

Austin, W.E.N., Hibbert, F.D., Rasmussen, S.O., Peters, C., Abbott, P.M., Bryant, C.L., 2012. The synchronization of palaeoclimatic events in the North Atlantic region during Greenland Stadial 3 (ca 27.5 to 23.3 kyr b2k). Quat. Sci. Rev. 36, 154–163.

637 Bahr, A., Jiménez-Espejo, F.J., Kolasinac, N., Grunert, P., Hernández-Molina, F.J., Röhl, U.,
638 Voelker, A.H.L., Escutia, C., Stow, D.A.V., Hodell, D., Alvarez-Zarikian, C.A., 2014.
639 Deciphering bottom current velocity and paleoclimate signals from contourite deposits in the
640 Gulf of Cádiz during the last 140 kyr: an inorganic geochemical approach. Geochem. Geophys.
641 Geosyst. 15, 3145–3160.
642
643 Bahr, A., Kaboth, S., Jiménez-Espejo, F.J., Sierro, F.J., Voelker, A.H.L., Lourens, L., Röhl, U.,
644 Reichart, G.J., Escutia, C., Hernández-Molina, F.J., Pross, J., Friedrich, O., 2015. Persistent
645 monsoonal forcing of Mediterranean Outflow Water dynamics during the late Pleistocene.
646 Geology 43 (11), 951-954.
647
648 Bard, E., Rostek, R., Turon, J.L., Gendreau, S., 2000. Hydrological impact of Heinrich events in
649 the subtropical northeast Atlantic. Science 289, 1321-1324.
650
651 Bard, E., Rostek, F., Ménot-Combes, G., 2004. Radiocarbon calibration beyond 20,000 14C yr
652 B.P. by means of planktonic foraminifera of the Iberian Margin. Quaternary Research 61, 204-
653 214.
654
655 Bar-Matthews, M., Ayalon, A., Kaufman, A., 2000. Timing and hydrological conditions of
656 Sapropel events in the Eastern Mediterranean, as evident from speleothems, Soreq cave. Isr.
657 Chem. Geol. 169 (1-2), 145-156.
658
659 Bar-Matthews, M., Ayalon, A., Gilmour, M., Matthews, A., Hawkesworth, C.J., 2003. Sea-land
660 oxygen isotopic relationships from planktonic foraminifera and speleothems in the Eastern
661 Mediterranean region and their implication for paleorainfall during interglacial intervals.
662 Geochim. Cosmochim. Acta 67 (17), 3181-3199.
663
664 Barker, S., Diz, P., Vautravers, M.J., Pike, J., Knorr, G. Hall, I.R., Broecker, W.S., 2009.
665 Interhemispheric Atlantic seesaw response during the last deglaciation. Nature 457 (7233), 1097-
666 1102.
667
668 Behrenfeld, M.J., Boss, E., Siegel, D.A., Shea, D.M., 2005. Carbon-based ocean productivity and
669 phytoplankton physiology from space. Glob. Biogeochem. Cycles 19, GB1006.
670 doi:10.1029/2004GB002299.
671
672 Berger, A., Loutre, M.F., 1991. Insolation values for the climate of the last 10 million years.
673 Quaternary Science Reviews 10 (4), 297-317.
674
675 Biebow, N., 1996. Dinoflagellatenzysten als Indikatoren der spätund postglazialen Entwicklung
676 des Auftriebsgeschehens vor Peru. Geomar Report 57, 100 pp.
677
678 Bouimetarhan, I., Marret, F., Dupont, L., Zonneveld, K., 2009. Dinoflagellate cyst distribution in
679 marine surface sediments off West Africa (6-17°N) in relation to sea-surface conditions,
680 freshwater input and seasonal coastal upwelling. Marine Micropaleontology 71, 113-130.
681
682 Bout-Roumazeilles, V., Combourieu Nebout, N., Peyron, O., Cortijo, E., Landais, A., Masson-
683 Delmotte, V., 2007. Connection between South Mediterranean climate and North African
684 atmospheric circulation during the last 50,000 yr BP North Atlantic cold events. Quaternary
685 Science Reviews 26 (25-28), 3197-3215.

Caballero, I., Morris, E.P., Prieto, L., Navarro, G., 2014. The influence of the Guadalquivir River on the spatio-temporal variability of suspended solids and chlorophyll in the Eastern Gulf of Cadiz. Medit. Mar. Sci. 15 (4), 721-738.

Cabeçadas, G., Brogueira, M.J., Goncalves, C., 2002. The chemistry of Mediterranean outflow and its interactions with surrounding waters. Deep Sea Research Part II: Topical Studies in Oceanography 49, 4263-4270.

Cabeçadas, G., Brogueira, M.J., Gonçalves, C., 2003. Intermediate water masses off south-southwest Portugal: Chemical tracers. Journal of Marine Research 61, 539-552.

Cacho, I., Grimalt, J.O., Sierro, F.J., Shackleton, N.J., Canals, M., 2000. Evidence for enhanced Mediterranean thermohaline circulation during rapid climatic coolings. Earth and Planetary Science Letters 183(3-4), 417-429.

Combourieu-Nebout, N., Paterne, M., Turon, J.L., Siani, G., 1998. A high resolution record of the last deglaciation in the central Mediterranean Sea : palaeovegetation and palaeohydrological evolution. Quaternary Science Reviews 17, 303-317.

Combourieu Nebout, N., Londeix, L., Baudin, F., Turon, J.L., von Grafenstein, R., Zahn, R., 1999. Quaternary marine and continental paleoenvironments in the western Mediterranean (site 976, Alboran sea): Palynological evidence. Proceedings of the Ocean Drilling Program, Scientific results 161, 457-468.

Combourieu-Nebout, N., Turon, J.L., Zahn, R., Capotondi, L., Londeix, L., Pahnke, K., 2002. Enhanced aridity and atmospheric high-pressure stability over the western Mediterranean during the North Atlantic cold events of the past 50 k.y. Geology 30, 863-866.

Dale, B., 1996. Dinoflagellate cyst ecology: modeling and geological applications. In: J. Jansonius and D.C. McGregor (Editors), Palynology: principles and applications, Vol. 3. AASP Foundation, Salt Lake City, 1 249-1 275.

Dansgaard, W., Johnsen, S.J., Clausen, H.B., Dahl-Jensen, D., Gundestrup, N.S., Hammer, C.U., Hvidberg, C.S., Steffenson, J.P., Sveinbjörnsdottir, A.E., Jouzel, J., Bond, G., 1993. Evidence for general instability of past climate from a 250-kyr ice-core record. Nature 364, 218-220.

de Abreu, L., Shackleton, N.J., Schönfeld, J., Hall, M., Chapman, M., 2003. Millennial-scale oceanic climate variability off the western Iberian margin during the last two glacial periods. Marine Geology 196, 1-20.

de Haas, H., Mienis, F., Frank, N., Richter, T.O., Steinbacher, R., de Stigter, H., van der Land, C., van Weering, T.C.E., 2009. Morphology and sedimentology of (clustered) cold-water coral mounds at the south Rockall Trough margins, NE Atlantic Ocean. Facies 55, 1-26.

de Leeuw, J.W., Versteegh, G.J.M., van Bergen, P.F., 2006. Biomacromolecules of algae and plants and their fossil analogues. Plant Ecology 182, 209-233.

deMenocal, P., Ortiz, J., Guilderson, T., Adkins, J., Sarnthein, M., Baker, L., Yarusinsky, M., 2000. Abrupt onset and termination of the African Humid Period: rapid climate responses to gradual insolation forcing. Quaternary Science Reviews 19, 347-361.

de Vernal, A., Henry, M., Bilodeau, G., 1999. Technique de préparation et d'analyse en micropaléontologie. Les Cahiers du GEOTOP vol. 3, Université du Québec à Montréal, Montréal, Canada.

de Vernal, A., Henry, M., Matthiessen, J., Mudie, P.J., Rochon, A., Boessenkool, K.P., Eynaud, F., Grøsfjeld, K., Guiot, J., Hamel, D., Harland, R., Head, M.J., Kunz-Pirrung, M., Levac, E., Loucheur, V., Peyron, O., Pospelova, V., Radi, T., Turon, J.L., Voronina, E., 2001. Dinoflagellate cyst assemblages as tracers of sea-surface conditions in the Northern North Atlantic, Arctic and sub-Arctic seas: The new 'n = 677' data base and its application for quantitative palaeoceanographic reconstruction. Journal of Quaternary Sciences 16, 681-698.

de Vernal, A., Eynaud, F., Henry, M., Hillaire-Marcel, C., Londeix, L., Mangin, S., Matthiessen, J., Marret, F., Radi, T., Rochon, A., Solignac, S., Turon, J.L., 2005. Reconstruction of sea-surface conditions at middle to high latitudes of the Northern Hemisphere during the last glacial maximum (LGM) based on dinoflagellate cyst assemblages. Quat. Sci. Rev. 24, 897-924.

de Vernal, A., Marret, F., 2007. Organic-walled dinoflagellates : tracers of sea-surface conditions, In Hillaire-Marcel and de Vernal (eds.) Proxies in Late Cenozoic Paleoceanography, Elsevier, 371-408.

Dodge, J.D., Harland, R., 1991. The distribution of planktonic dinoflagellates and their cysts in the eastern and north-eastern Atlantic Ocean. New Phytol. 118, 593-603.

Dorschel, B., Hebbeln, D., Rüggeberg, A., Dullo, W.C., 2005. Growth and erosion of a cold-water coral covered carbonate mound in the Northeast Atlantic during the Late Pleistocene and Holocene. Earth Planet. Sci. Lett. 233, 33-44.

Eisele, M., Hebbeln, D., Wienberg, C., 2008. Growth history of a cold-water coral covered carbonate mound – Galway Mound, Porcupine Seabight. NE-Atlantic Mar. Geol. 253, 160-169.

Eynaud, F., Turon, J.L., Sánchez-Goñi, M.F., Gendreau, S., 2000. Dinoflagellate cyst evidence of "Heinrich-like events" off Portugal during the marine isotopic stage 5. Mar. Micropal. 40, 9-21.

Eynaud, F., de Abreu, L., Voelker, A., Schönfeld, J., Salgueiro, E., Turon, J.L., Penaud, A., Toucanne, S., Naughton, F., Sánchez-Goñi, M.F., Malaizé, B., Cacho, I., 2009. Position of the Polar Front along the western Iberian margin during key cold episodes of the last 45 ka. Geochem. Geophys. Geosyst. 10, Q07U05, doi:10.1029/2009GC002398.

Eynaud, F., Londeix L., Penaud A., Sánchez-Goñi M.F., Oliveira D., Desprat S., Turon J.L., 2016. Dinoflagellate cyst population evolution throughout past interglacials: key features along the Iberian margin and insights from the new IODP Site U1385 (Exp 339). Global and Planetary Change 136, 52-64.

Falkowski, P.G., Raven, J.A. 1997. Aquatic Photosynthesis. Blackwell Science, London, 375 pp.

Fasham, M.J.R., Platt, T., Irwin, B., Jones, K., 1985. Factors affecting the spatial pattern of the Deep Chlorophyll Maximum in the region of the Azores Front, In: Crease, J., Gould, W.J., Saunders, P.M. (Eds.), Essays On Oceanography: A Tribute to John Swallow. Progress in Oceanography 14, Pergamon, Oxford, 129-166.

Fatela, F., Taborda, R., 2002. Confidence limits of species proportions in microfossil assemblages, Mar. Micropaleontol. 45, 169-174.

Fensome, R.A., Williams, G.L., 2004. The Lentin and Williams index of fossil dinoflagellates, 2004 edition. AASP Foundation Contributions Series 42, 909 pp.

Fensome, R.A., MacRae, R.A., Williams, G.L., 2008. DINOFLAJ2, Version1. American Association of Stratigraphic Palynologists (DataSeries no. 1). Available at: dinoflaj.smu.ca/wiki/Main_Page.

Flecha, S., Perez, F.F., Navarro, G., Ruiz, J., Olive, I., Rodriguez-Galvez, S., Costas, E., Huertas, I. E., 2012. Anthropogenic carbon inventory in the Gulf of Cadiz. J. Mar. Syst. 92, 67-75.

Fletcher, W.J., Sánchez-Goñi M.F., 2008. Orbital- and sub-orbital scale climate impacts on vegetation of the western Mediterranean basin over the last 48,000 yr. Quat. Res. 70, 451-464.

Frank, N., Lutringer, A., Paterne, M., Blamart, D., Henriet, J.-P., van Rooij, D., van Weering, T.C.E., 2005. Deep-water corals of the northeastern Atlantic margin: carbonate mound evolution and upper intermediate water ventilation during the Holocene. In: Freiwald, A., Roberts, J.M. (Eds.), Cold-water Corals and Ecosystems. Springer, Heidelberg, pp. 113-133.

Frank, N., Ricard, E., Lutringer-Paque, A., van der Land, C., Colin, C., Blamart, D., Foubert, A., Van Rooij, D., Henriet, J.-P., de Haas, H., van Weering, T.C.E., 2009. The Holocene occurrence of cold-water corals in the NE Atlantic: implications for coral carbonate mound evolution. Mar. Geol. 266, 129-142.

Freiwald, A., Fosså, J.H., Grehan, A., Koslow, T., Roberts, J.M., 2004. Cold-water Coral Reefs. UNEP-WCMC, Biodiversity Series 22, Cambridge, UK, pp. 84.

Frigola, J., Moreno, A., Cacho, I., Canals, M., Sierro, F.J., Flores, J.A., Grimalt, J.O., 2008. Evidence of abrupt changes in Western Mediterranean Deep Water circulation during the last 50 kyr: A high-resolution marine record from the Balearic Sea. Quaternary International 181 (1), 88-104.

Gasse, 2000. Hydrological changes in the African tropicssince the Last Glacial Maximum. Quaternary Science Reviews 19, 189-211.

Gherardi, J.M., Labeyrie, L., McManus, J.F., Francois, R., Skinner, L.C., Cortijo, E., 2005. Evidence from the northeastern Atlantic basin for variability in the rate of the meridional overturning circulation through the last deglaciation. Earth and Planetary Science Letters 240, 710-723.

Gómez, F., González, N., Echevarría, F., García, C.M., 2000. Distribution and Fluxes of Dissolved Nutrients in the Strait of Gibraltar and its Relationships to Microphytoplankton Biomass. Estuarine, Coastal and Shelf Science 51 (4), 439-449.

Gould, W.J. 1985. Physical oceanography of the Azores Front, in: J. Crease, W.J. Gould, P.M. Saunders (Eds.), Essays in oceanography: A Tribute to John Swallow, Progress in Oceanography, Pergamon, Oxford, 1985, pp. 167-190.

Grootes, P.M., Stuiver, M., White, J.W.C., Johnsen, S., Jouzel, J., 1993. Comparison of oxygen isotope records from the GISP2 and GRIP Greenland ice cores. Nature 366, 552-554.

Grootes, P.M., Stuiver, M., 1997. Oxygen 18/16 variability in Greenland snow and ice with 103 to 105-year time resolution. Journal of Geophysical Research 102, 26,455-26,470.

Guiot, J., de Vernal, A., 2007. Transfer functions: methods for quantitative paleoceanography based on microfossils, In Hillaire-Marcel and de Vernal (eds.) Proxies in Late Cenozoic Paleoceanography, Elsevier, pp. 523-563.

Habgood, E.L., Kenyon, N.H., Masson, D.G., Akhmetzhanov, A., Weaver, P.P.E., Gardner, J., Mulder, T., 2003. Deep-water sediment wave fields, bottom current sand channels and gravity flow channellobe systems: Gulf of Cadiz, NE Atlantic. Sedimentology 50, 483-510.

Hammer, Ø., Harper, D.A.T., Ryan, P.D., 2001. Past: Paleontological Statistics Software Package for Education and Data Analysis. Palaeontologia Electronica, vol. 4, issue 1, art. 4: 9pp., 178kb. http://palaeo-electronica.org/2001_1/past/issue1_01.htm.

Hardy, W., Penaud, A., Marret, F., Bayon, G., Marsset, T., Droz, L., 2016. Dinocyst assemblage constraints on oceanographic and atmospheric processes in the eastern equatorial Atlantic over the last 44 kyr. Biogeosciences 13, 4823-4841.

Harper, D.A.T. (ed.). 1999. Numerical Palaeobiology. John Wiley & Sons, Chichester.

Haynes, R., Barton, E.D., Pilling, I., 1993. Development, persistence, and variability of upwelling filaments off the Atlantic coast of the Iberian Peninsula. J. Geophys. Res. 98 (C12), 22,681-22,692.

Head, M.J., 1996. Modern dinoflagellate cysts and their biological affinities. In "Palynology: principles and Applications. Chapter 30." (Jansonius, J., and McGregor, D.C., editors), AASP Foundation, 1,197-1,248.

Hernández-Molina, F.J., Stow, D.A.V., Alvarez-Zarikian, C.A., Acton, G., Bahr, A., Balestra, B., Ducassou, E., Flood, R., Flores, J.-A., Furota, S., Grunert, P., Hodell, D., Jimenez-Espejo, F., Kim, J.K., Krissek, L., Kuroda, J., Li, B., Llave, E., Lofi, J., Lourens, L., Miller, M., Nanayama, F., Nishida, N., Richter, C., Roque, C., Pereira, H., Sánchez-Goñi, M.F., Sierro, F.J., Singh, A.D., Sloss, C., Takashimizu, Y., Tzanova, A., Voelker, A., Williams, T., Xuan, C., 2014. Onset of Mediterranean Outflow into the North Atlantic. Science 344, 1244-1250.

Holzwarth, U., Meggers, H., Esper, O., Kuhlmann, H., Freudenthal, T., Hensen, C., Zonneveld, K.A.F., 2010. NW African climate variations during the last 47,000 years: Evidence from

organic-walled dinoflagellate cysts. Palaeogeography, Palaeoclimatology, Palaeoecology 291 (3-4), 443-455.

Hsu, C.P.F., Wallace, J.M., 1976. The global distribution in annual and semiannual cycles in precipitation. Monthly Weather Review 104 (9), 1093-1101.

Huertas, I.E., Navarro, G., Rodriguez-Galvez, S., Lubian, L.M., 2006. Temporal patterns of carbon dioxide in relation to hydrological conditions and primary production in the northeastern shelf of the Gulf of Cadiz (SW Spain). Deep-Sea Research II 53, 1,344-1,362.

Huertas, I. E., Rios, A.F., Garcia-Lafuente, J., Makaoui, A., Rodriguez-Galvez, S., Sanchez-Roman, A., Orbi, A., Ruiz, J., Perez, F.F., 2009. Anthropogenic and natural CO2 exchange through the Strait of Gibraltar. Biogeosciences 6, 647-662.

Ivanovic, R.F., Valdes, P.J., Flecker, R., Gregoire, L.J., Gutjahr, M., 2013. The parameterisation of Mediterranean-Atlantic water exchange in the Hadley Centre model HadCM3, and its effect on modelled North Atlantic climate. Ocean Modelling 62, 11-16.

Kaboth, S., Bahr, A., Reichart, G.J., Jacobs, B., Lourens, L.J., 2015. New insights into upper MOW variability over the last 150 kyr from IODP 339 site U1386 in the Gulf of Cadiz. Marine Geology, doi: 10.1016/j.margeo.2015.08.014.

Kallel, N., Paterne, M., Duplessy, J. C., Vergnaud-Grazzini, C., Pujol, C., Labeyrie, L., Arnold, M., Fontugne, M., Pierre, C., 1997. Enhanced rainfall in the Mediterranean region during the last sapropel event. Oceanologica Acta 20, 697-712.

Kodrans-Nsiah, M., de Lange, G.J., Zonneveld, K.A.F., 2008. A natural exposure experiment on short-term species-selective aerobic degradation of dinoflagellate cysts. Review of Palaeobotany and Palynology 152 (1-2), 32-39.

Labeyrie, L., Jansen, E., Cortijo, 2003. Les rapports de campagnes à la mer. MD 114/IMAGES V OCE/2003/02. Brest, Institut Polaire Francais-Paul Emile Victor, 850 pp.

Lebreiro, S.M., Moreno, J.C., Abrantes, F.F., Pflaumann, U., 1997. Productivity and paleoceanographic implications on the Tore Seamount (Iberian Margin) during the last 225 kyr: Foraminiferal evidence. Paleoceanography 12 (5), 718-727.

Le Mézo, P., Kageyama, M., Bopp, L., Beaufort, L., 2015. Mechanisms behind primary production distribution during the last glacial-interglacial cycle. Geophysical Research Abstracts Vol. 17, EGU2015-880.

Lewis, J., Dodge, J.D., Powell, A.J., 1990. Quaternary dinoflagellate cysts from the upwelling system off shore Peru, Hole 686B, ODP leg 112. Proc. ODP Sci. Results 112, 323-327.

Lofi, J., Voelker, A.H.L., Ducassou, E., Hernández-Molina, F.J., Sierro, F.J., Bahr, A., Galvani, A., Lourens, L.J., Pardo-Igúzquiza, E., Pezard, P., Rodríguez-Tovar, F.J., Williams, T., 2016. Quaternary chronostratigraphic framework and sedimentary processes for the Gulf of Cadiz and Portuguese Contourite Depositional Systems derived from Natural Gamma Ray records. Marine Geology 377, 40-57.

Londeix, L., Benzakour, M., Suc, J.-P., Turon, J.L., 2007. Messinian palaeoenvironments and hydrology in Sicily (Italy): The dinoflagellate cyst record. Geobios 40, 233-250.

Lourens, L.J., Antonarakou, A., Hilgen, F.J., Van Hoof, A.A.M., Vergnaud-Grazzini, C., Zachariasse, W.J., 1996. Evaluation of the Plio-Pleistocene astronomical timescale. Paleoceanography 11 (4), 391-413.

Lourens, L.J., Wehausen, R., Brumsack, H.J., 2001. Geological constraints on tidal dissipation and dynamical ellipticity of the Earth over the past three million years. Nature 409, 1029-1033.

Macías, D., Guerreiro, C.T., Prieto, L., Peliz, A., Ruiz, J., 2014. A high-resolution hydrodynamic-biogeochemical coupled model of the Gulf of Cadiz - Alboran Sea region. Medit. Mar. Sci. 15, 739-752.

Magny, M., Combourieu-Nebout, N., de Beaulieu, J. L., Bout-Roumazeilles, V., Colombaroli, D., Desprat, S., Francke, A., Joannin, S., Ortu, E., Peyron, O., Revel, M., Sadori, L., Siani, G., Sicre, M. A., Samartin, S., Simonneau, A., Tinner, W., Vannière, B., Wagner, B., Zanchetta, G., Anselmetti, F., Brugiapaglia, E., Chapron, E., Debret, M., Desmet, M., Didier, J., Essallami, L., Galop, D., Gilli, A., Haas, J. N., Kallel, N., Millet, L., Stock, A., Turon, J. L., Wirth, S., 2013. Northesouth palaeohydrological contrasts in the central Mediterranean during the Holocene: tentative synthesis and working hypotheses. Clim. Past 9, 2043-2071.

Mariotti, V., Bopp, L., Tagliabue, A., Kageyama, M, Swingedouw, D., 2012. Marine productivity response to Heinrich events: a model-data comparison. Clim. Past Discuss. 8, 557-594.

Marret, F., 1994. Distribution of dinoflagellate cysts in recent marine sediments from the east Equatorial Atlantic (Gulf of Guinea). Review of Palaeobotany and Palynology 84, 1-22.

Marret, F., Turon, J.L., 1994. Paleohydrology and paleoclimatology off Northwest Africa during the last glacial-interglacial transition and the Holocene: Palynological evidences. Marine Geology 118, 107-117.

Marret, F., Zonneveld, K.A.F., 2003. Atlas of modern organic-walled dinoflagellate cyst distribution. Review of Palaeobotany and Palynology 125, 1-200.

McManus, J.F., Keigwin, L., Francois, R., Drown-Leger, S., Gherardi, J.M., 2004. Collapse and rapid resumption of Atlantic meridional circulation linked to deglacial climate changes. Nature 428, 834-837.

Mercone, D., Thomson, J. Croudace, I.W. Siani, G. Paterne, M. Troelstra, S., 2000. Duration of S1, the most recent sapropel in the eastern Mediterranean Sea, as indicated by accelerator mass spectrometry radiocarbon and geochemical evidence. Paleoceanography 15, 336-347.

Mertens, K.N., Verhoeven, K., Verleye, T., Louwye, S., Amorim, A., Ribeiro, S., Deaf, A.S., Harding, I. C., De Schepper, S., Gonzalez, C., Kodrans-Nsiah, M., De Vernal, A., Henry, M., Radi, T., Dybkjaer, K., Poulsen, N.E., Feist-Burkhardt, S., Chitolie, J., Heilmann-Clausen, C., Londeix, L., Turon, J.L., Marret, F., Matthiessen, J., McCarthy, F.M.G., Prasad, V., Pospelova, V., Kyffin Hughes, J.E., Riding, J.B., Rochon, A., Sangiorgi, F., Welters, N., Sinclair, N., Thun,

C., Soliman, A., Van Nieuwenhove, N., Vink, A., Young, M., 2009. Determining the absolute abundance of dinoflagellate cysts in recent marine sediments: The Lycopodium marker-grain method put to the test. Review of Palaeobotany and Palynology 157, 238-252.

Mikolajewicz, 2011. Modeling Mediterranean Ocean climate of the Last Glacial Maximum. Clim. Past 7, 161-180.

Moreno, A., Cacho, I., Canals, M., Prins, M.A., Sánchez-Goñi, M.F., Grimalt, J.O., Weltje, G.J., 2002. Saharan dust transport and high-latitude glacial climatic variability: The Alboran Sea record. Quaternary Research 58 (3), 318-328.

Moreno, A., Cacho, I., Canals, M., Grimalt, J.O., Sánchez-Goñi, M.F., Shackleton, N.J., Sierro, F.J., 2005. Links between marine and atmospheric processes oscillating on a millennial time-scale. A multiproxy study of the last 50,000 yr from the Alboran Sea (Western Mediterranean Sea). Quaternary Science Reviews 24, 1623-1636.

Naughton, F., Bourillet, J.F., Sánchez-Goñi, M.F., Turon, J.L., Jouanneau, J.M., 2007. Long-term and millennial-scale climate variability in northwestern France during the last 8850 years. The Holocene 17 (7), 939-953.

Navarro, G., Ruiz, J., 2006. Spatial and temporal variability of phytoplankton in the Gulf of Cadiz through remote sensing images. Deep-Sea Res. II 53, 1,241-1,260.

Pailler, D., Bard, E., 2002. High frequency palaeoceanographic changes during the past 140 000 yr recorded by the organic matter in sediments of the Iberian Margin. Palaeogeography, Palaeoclimatology, Palaeoecology 181 (4), 431-452.

Patton, G.M., Martin, P.A., Voelker, A., Salgueiro, E., 2011. Multiproxy comparison of oceanographic temperature during Heinrich Events in the eastern subtropical Atlantic. Earth and Planetary Science Letters 310 (1-2), 45-58.

Peliz, A., Dubert, J., Santos, A., Oliveira, P., Le Cann, B., 2005. Winter upper ocean circulation in the Western Iberian Basin-Fronts, eddies and poleward flows: An overview. Deep Sea Res. I 52, 621-646.

Peliz, A., Marchesiello, P., Santos, A.M.P., Dubert, J., Teles-Machado, A., Marta-Almeida, M., Le Cann, B., 2009. Surface circulation in the Gulf of Cadiz: 2. Inflow-outflow coupling and the Gulf of Cadiz Slope Current. J. Geophys. Res. 114, C03011. http://dx.doi.org/10.1029/2008JC004771 16 pages.

Penaud, A., Eynaud, F., Turon, J.L., Zaragosi, S., Marret, F., Bourillet, J.F., 2008. Interglacial variability (MIS 5 and MIS 7) and dinoflagellate cyst assemblages in the Bay of Biscay (North Atlantic). Marine Micropaleontology 68, 136-155.

Penaud, A., Eynaud, F., Turon, J.L., Zaragosi, S., Malaizé, B., Toucanne, S., Bourillet, J.F., 2009. What forced the collapse of European ice sheets during the last two glacial periods (150 ka B.P. and 18 ka cal B.P.)? Palynological evidence. Palaeogeography, Palaeoclimatology, Palaeoecology 281, 66-78.

Penaud, A., Eynaud, F., Turon, J.L., Blamart, D., Rossignol, L., Marret, F., Lopez-Martinez, C., Grimalt, J.O., Malaizé, B., Charlier, K., 2010. Contrasting Heinrich Events 1, 2, and LGM conditions off Morocco: Paleoceanographical evidences of warmer LGM and colder HE 1. Quaternary Science Reviews 29 (15-16), 1,923-1,939.

Penaud, A., Eynaud, F., Voelker, A., Kageyama, M., Marret, F., Turon, J.L., Blamart, D., Mulder, T., Rossignol, L., 2011a. Assessment of sea surface temperature changes in the Gulf of Cadiz during the last 30 ka: implications for glacial changes in the regional hydrography. Biogeosciences 8, 2,295-2,316.

Penaud, A., Eynaud, F., Malaizé, B., Sánchez-Goñi, M., Turon, J.L., Rossignol, L., 2011b. Contrasting sea-surface responses between western Mediterranean Sea and eastern subtropical latitudes of the North Atlantic during the abrupt climatic events of MIS 3. Marine Micropaleontology 80 (1-2), 1-17.

Radi, T., de Vernal, A., 2008. Dinocysts as proxy of primary productivity in mid–high latitudes of the Northern Hemisphere. Mar. Micropaleontol. 68, 84-114.

Rasmussen, S.O., Bigler, M., Blockley, S.P., Blunier, T., Buchardt, S.L., Clausen, H.B., Cvijanovic, I., Dahl-Jensen, D., Johnsen, S.J., Fischer, H., Gkinis, V., Guillevic, M., Hoek, W.Z., Lowe, J.J., Pedro, J.B., Popp, T., Seierstad, I.K., Steffensen, J.P., Svensson, A.M., Vallelonga, P., Vinther, B.M., Walker, M.J.C., Wheatley, J.J., Winstrup, M., 2014. A stratigraphic framework for abrupt climatic changes during the Last Glacial period based on three synchronized Greenland ice-core records: refining and extending the INTIMATE event stratigraphy. Quaternary Science Reviews 106, 14-28.

Reimer, P.J., Bard, E., Bayliss, A., Beck, J.W., Blackwell, P.G., Bronk Ramsey, C., Buck, C.E., Cheng, H., Edwards, R.L., Friedrich, M., Grootes, P.M., Guilderson, T.P., Haflidason, H., Hajdas, I., Hatte, C., Heaton, T.J., Hogg, A.G., Hughen, K.A., Kaiser, K.F., Kromer, B., Manning, S.W., Niu, M., Reimer, R.W., Richards, D.A., Scott, E.M., Southon, J.R., Turney, C.S.M., van der Plicht, J., 2013. IntCal13 and Marine13 radiocarbon age calibration curves 0-50,000 years cal BP. Radiocarbon 55, 1869–1887.

Rochon, A., de Vernal, A., Turon, J.L., Matthiessen, J., Head, M.J., 1999. Distribution of Recent Dinoflagellate cysts in surface sediments from the North Atlantic Ocean and adjacent seas in relation to sea-surface parameters. Am. Assoc. of Stratigr. Palynol. AASP Contr. Ser. 35, 1-152.

Rogerson, M., Rohling, E.J., Weaver, P.P.E., Murray, J.W., 2004. The Azores Front since the Last Glacial Maximum. Earth and Planetary Science Letters 222, 779-789.

Rogerson, M., Colmenero-Hidalgo, E., Levine, R. C., Rohling, E. J., Voelker A. H. L., Bigg, G. R., Schönfeld, J., Cacho, I., Sierro, F. J., Löwemark, L., Reguera, M. I., de Abreu, L., Garrick, K., 2010. Enhanced Mediterranean-Atlantic exchange during Atlantic freshening phases, Geochem. Geophys. Geosyst. 11, Q08013, doi:10.1029/2009GC002931.

Rogerson, M., Schönfeld, J., Leng, M.J., 2011. Qualitative and quantitative approaches in palaeohydrography: A case study from core-top parameters in the Gulf of Cadiz. Marine Geology 280 (1-4), 150-167.

Rogerson, M., Rohling, E.J., Bigg, G.R., Ramirez., J., 2012. Paleoceanography of the Atlantic-Mediterranean exchange: overview and first quantitative assessment of climatic forcing. Rev. Geophys. 50, RG2003, doi: 10.1029/2011RG000376.

Rohling, E.J., Hilgen, F.J., 1991. The eastern Mediterranean climate at times of sapropel formation: a review. Geol. Mijnb. 70, 253-264.

Rossignol-Strick, M., 1983. African monsoons, an immediate climate response to orbital insolation. Nature 30, 446-449.

Rudnick, D.L., 1996. Intensive surveys of the Azores Front: 2. Inferring the geostrophic and vertical velocity fields. Journal of Geophysical Research 101 (C7), 16,291-16,303.

Rüggeberg, A., Dullo, W.C., Dorschel, B., Hebbeln, D., 2007. Environmental changes and growth history of a cold-water carbonate mound (Propeller Mound, Porcupine Seabight). Int. J. Earth Sci. 96, 57-72.

Sabine, C.L., Feely, R.A., Watanabe, Y.W., Lamb, M., 2004. Temporal evolution of the North Pacific CO2 uptake rate. Journal of Oceanography 60 (3), 5-15.

Salgueiro, E., Voelker, A.H.L., de Abreu, L., Abrantes, F., Meggers, H., Wefer, G., 2010. Temperature and productivity changes off the western Iberian margin during the last 150 ky. Quaternary Science Reviews 29, 680-695.

Salgueiro, E., Naughton, F., Voelker, A.H.L., de Abreu, L., Alberto, A., Rossignol, L., Duprat, J., Magalhães, V.H., Vaqueiro, S., Turon, J.L., Abrantes, F., 2014. Past circulation along the western Iberian margin: a time slice vision from the Last Glacial to the Holocene.Quat. Sci. Rev. 106, 316-329.

Sánchez-Goñi, M.F., Turon, J.L., Eynaud, F., Gendreau, S., 2000. European climatic response to millennial-scale changes in the atmosphere-ocean system during the Last Glacial Period. Quat. Res. 54, 394-403.

Sánchez-Goñi, M.F., Cacho, I., Turon, J.L., Guiot, J., Sierro, F., Peypouquet, J.P., Grimalt, J.O., Shackleton, N.J., 2002. Synchronicity between marine and terrestrial responses to millennial scale climatic variability during the last glacial period in the Mediterranean region. Climate Dynamics 19 (1), 95-105.

Sánchez-Goñi, M.F., Harrison, S.P., 2010. Millennial-scale climate variability and vegetation changes during the Last Glacial: Concepts and terminology. Quaternary Science Reviews 29 (21-22), 2,823-2,827.

Schmittner, A., 2005. Decline of the marine ecosystem caused by a reduction in the Atlantic overturning circulation. Nature 434, 628-633.

Shackleton, N.J, Hall, M.A., Vincent, E., 2000. Phase relationships between millennial-scale events 64,000-24,000 years ago. Paleoceanography 15(6), 565-569.

Sierro, F.J., Ledesma, S., Flores, J.-A., Torrescusa, S., del Olmo, W.M., 2000. Sonic and gamma-ray astrochronology: Cycle to cycle calibration of Atlantic climatic records to Mediterranean sapropels and astronomical oscillations. Geology 28, 695-698.

Sierro, F.J., Hodell, D.A., Curtis, J.H., Flores, J.A., Reguera, I., Colmenero-Hidalgo, E., Barcena, M.A., Grimalt, J.O., Cacho, I., Frigola, J., Canals, M., 2005. Impact of iceberg melting on Mediterranean thermohaline circulation during Heinrich events. Paleoceanography 20, PA2019, 1-13.

Stockmarr, J., 1971. Tablets with spores used in absolute pollen analysis. Pollen et Spores 13, 615-621.

Stuiver, M., Reimer, P.J., 1993. Extended 14C database and revised CALIB radiocarbon calibration program. Radiocarbon 35, 215-230.

Svensson, A., Andersen, K.K., Bigler, M., Clausen, H.B., Dahl-Jensen, D., Davies, S.M., Johnsen, S.J., Muscheler, R., Parrenin, F., Rasmussen, S.O., Röthlisberger, R., Seierstad, I., Steffensen, J.P., Vinther, B.M., 2008. A 60 000 year Greenland stratigraphic ice core chronology. Clim. Past 4, 47-57.

Takahashi, T., Sutherland, S.C., Wanninkhof, R., Sweeney, C., Feely, R.A., Chipman, D.W., Hales, B., Friederich, G., Chavez, F., Sabine, C., Watson, A., Bakker, D.C.E., Schuster, U., Metzl, N., Yoshikawa-Inoue, H., Ishii, M., Midorikawa, T., Nojiri, Y., Körtzinger, A., Steinhoff, T., Hoppema, M., Olafsson, J., Arnarson, T.S., Tilbrook, B., Johannessen, T., Olsen, A., Bellerby, R., Wong, C.S., Delille, B., Bates, N.R., de Baar, H.J.W., 2009. Climatological mean and decadal change in surface ocean pCO2, and net sea-air CO2 flux over the global oceans. Deep-Sea Research II 56 (8-10), 554-577.

Targarona, J., Warnaar, J., Boessenkool, K.P., Brinkhuis, H., Canals, M., 1999. Recent dinoflagellate cyst distribution in the North Canary Basin, NW Africa. Grana 38, 170-178.

Toucanne, S., Mulder, T., Schönfeld, J., Hanquiez, V., Gonthier, E., Duprat, J., Cremer, M., Zaragosi, S., 2007. Contourites of the Gulf of Cadiz: A high-resolution record of the paleocirculation of the Mediterranean outflow water during the last 50,000 years. Palaeogeography, Palaeoclimatology, Palaeoecology 246 (2-4), 354-366.

Toucanne, S., Jouet, G., Ducassou, E., Bassetti, M.A., Dennielou, B., Minto'o, C.M.A, Lahmi, M., Touyet, N., Charlier, K., Lericolais, G., Mulder, T., 2012. A 130,000-year record of levantine intermediate water flow variability in the Corsica Trough, western Mediterranean Sea. Quat. Sci. Rev. 33, 55-73.

Toucanne, S., Angue Minto'o, C.M., Fontanier, C., Bassetti, M.A., Jorry, S.J., Jouet, G., 2015. Tracking rainfall in the northern Mediterranean borderlands during sapropel deposition. Quaternary Science Reviews, in press.

Tuenter, E., Weber, S.L., Hilgen, F.J., Lourens, L.J., 2003. The response of the African summer monsoon to remote and local forcing due to precession and obliquity. Glob. Planet. Change 36, 219-235.

Turon, J. L., 1984. Le palynoplancton dans l'environnement actuel de l'Atlantique Nord-oriental. Evolution climatique et hydrologique depuis le dernier maximum glaciaire. Mémoires de l'Institut de Géologie du Bassin d'Aquitaine 17, 313 pp.

Turon, J.L., Londeix, L., 1988. Les asssemblages de kystes de dinoflagellés en Méditerranée occidentale (Mer d'Alboran): mise en evidence de l'évolution des paléoenvironnement depuis le dernier maximum glaciaire. Bull. Centres Rech. Explor.-prod. Elf-Aquitaine 12, 313-344.

Turon, J.L., Lézine, A.M., Denèfle, M., 2003. Land-sea correlations for the last glaciation inferred from a pollen and dinocyst record from the Portuguese margin. Quaternary Research 59, 88-96.

Vautravers, M.J., Shackleton, N.J., 2006. Centennial-scale surface hydrology off Portugal during marine isotope stage 3: Insights from planktonic foraminiferal fauna variability. Paleoceanography 21, PA3004, doi:10.1029/2005PA001144.

Versteegh, G.J.M., 1994. Recognition of cyclic and non-cyclic environmental changes in the Mediterranean Pliocene; a palynological approach. Mar. Micropaleontol. 23, 147-171.

Voelker, A.H.L., Lebreiro, S.M., Schönfeld, J., Cacho, I., Erlenkeuser, H., Abrantes, F., 2006. Mediterranean outflow strengthening during northern hemisphere coolings: A salt source for the glacial Atlantic? Earth and Planetary Science Letters 245 (1-2), 39-55.

Voelker, A.H.L., de Abreu, L., Schönfeld, J., Erlenkeuser, H., Abrantes, F., 2009. Hydrographic Conditions Along the Western Iberian Margin During Marine Isotope Stage 2. Geochem. Geophys. Geosyst. 10(Q12U08), DOI: 10.1029/2009GC002605.

Voelker, A.H.L., Salgueiro, E., Rodrigues, T., Jimenez-Espejo, F.J., Bahr, A., Alberto, A., Loureiro, I., Padilha, M., Rebotima, A., Röhl, U., 2015. Mediterranean Outflow and surface water variability off southern Portugal during the early Pleistocene: A snapshot at Marine Isotope Stages 29 to 34 (1020–1135 ka). Global and Planetary Change 133, 223-237.

Wall, D., Dale, B., Lohmann, G.P., Smith, W.K., 1977. The environment and climatic distribution of dinoflagellate cysts in modern marine sediments from regions in the north and south Atlantic oceans and adjacent seas. Mar. Micropaleontol. 2, 121-200.

Warrick, J.A., Fong, D.A., 2004. Dispersal scaling from the world's rivers. Geophysical research letters 31, L04301, doi:10.1029/2003GL019114.

Wienberg, C., Hebbeln, D., Fink, H.G., Mienis, F., Dorschel, B., Vertino, A., López Correa, M., Freiwald, A., 2009. Scleractinian cold-water corals in the Gulf of Cádiz – first clues about their spatial and temporal distribution. Deep Sea Res. I 56, 1873-1893.

Wienberg, C., Frank, N., Mertens, K.N., Stuut, J.B., Marchant, M., Fietzke, J., Mienis, F., and Hebbeln, D., 2010. Glacial cold-water coral growth in the Gulf of Cádiz: Implications of increased palaeo-productivity: Earth and Planetary Science Letters. 298, 405-416.

Wolff, E.W., Chappellaz, J., Blunier, T., Rasmussen, S.O., Svensson, A., 2010. Millennial-scale variability during the last glacial: The ice core record. Quat. Sci. Rev. 29, 2828-2838.

Zanchetta, G., Drysdale, R.N., Hellstrom, J.C., Fallick, A.E., Isola, I., Gagan, M.K., Pareschi, M.T., 2007. Enhanced rainfall in the Western Mediterranean during deposition of sapropel S1: stalagmite evidence from Corchia cave (Central Italy). Quat. Sci. Rev. 26 (3-4), 279-286.

Zaragosi, S., Eynaud, F., Pujol, C., Auffret, G.A., Turon, J.L., Garlan, T., 2001. Initiation of European deglaciation as recorded in the north-western Bay of Biscay slope environments (Meriadzek Terrace and Trevelyan Escarpment): a multi-proxy approach. Earth Planet. Sci. Lett. 188, 493-507.

Zonneveld, K.A.F., Ganssen, G., Troelstra, S., Versteegh, G.J.M., Visscher, H., 1997a. Mechanisms forcing abrupt fluctuations of the Indian Ocean summer monsoon during the last deglaciation. Quat. Sci. Rev. 16, 187-201.

Zonneveld, K.A.F., Versteegh, G.J.M., De Lange, G.J., 1997b. Preservation of organic walled dinoflagellate cysts in different oxygen regimes: a 10,000 years natural experiment. Mar. Micropaleontol. 29, 393-405.

Zonneveld, K.A.F., Hoek, R.P., Brinkhuis, H., Willems, H., 2001. Geographical distributions of organic-walled dinoflagellate cysts in surficial sediments of the Benguela upwelling region and their relationship to upper ocean conditions. Progress in Oceanography 48, 25-72.

Zonneveld, K.A.F, Marret, F., Versteegh, G.J.M., Bogus, K., Bonnet, S., Bouimetarhan, I., Crouch, E., de Vernal, A., Elshanawany, R., Edwards, L., Esper, O., Forke, S., Grøsfjeld, K., Henry, M., Holzwarth, U., Kielt, J.F., Kim, S.Y., Ladouceur, S., Ledu, D., Chen, L., Limoges, A., Londeix, L., Lu, S.H., Mahmoud, M.S., Marino, G., Matsouka, K., Matthiessen, J., Mildenhal, D.C., Mudie, P.J., Neil, H.L., Pospelova, V., Qi, Y., Radi, T., Richerol, T., Rochon, A., Sangiorgi, F., Solignac, S., Turon, J.L., Verleye, T., Wang, Y., Wang, Z., Young, M., 2013. Atlas of modern dinoflagellate cyst distribution based on 2405 data points. Review of Palaeobotany and Palynology, 191, 1-197.

## 9. TABLE CAPTION

**Table 1**: Modern distribution *versus* past occurrences (MD99-2339 record) for selected major dinocyst species found in the fossil assemblage (cf. Figure 5).

## 10. FIGURE CAPTION

**Figure 1:** Area of interest with major sea-surface features. Study core MD99-2339, as well as other cores discussed in the paper, are located on the large map, depicting also the bathymetry of the study area and the major surface currents within the Alboran sea; WAG: Western Alboran Gyre; EAG: Eastern Alboran Gyre; AOF: Almeria-Oran Front; AC: Algerian Current. The small map on the left present large scale North Atlantic currents with: the North Atlantic Drift (NAD), the Portugal Current (PC) flowing southward from 45°N to 30°N, the Azores Current (AzC) derived from the southern branch of the Gulf Stream and flowing eastward to the Gulf of Cadiz at about 35°N, and the Canary Current (CC) fed by both the AzC and the PC. Together, these currents form the Eastern Boundary Current of the North Atlantic subtropical gyre.

**Figure 2:** a) Age-depth model for core MD99-2339 (all symbols are explained in the Figure), allowing to compare: b) the new age model (this study: planktonic $\delta^{18}O$ monospecific record in black) with the first published one (Voelker et al., 2006: planktonic $\delta^{18}O$ record in red).

**Figure 3:** Comparison, against age (new age model from this study), between the planktonic $\delta^{18}O$ monospecific record of core MD99-2339 (red curve, Voelker et al., 2006) and the NGRIP $\delta^{18}O$ according to the GICC05 time scale (Svensson et al., 2008). a) Red stars locate the 6 radiocarbon dates retained for the chronology of core MD99-2339, and dark arrows locate the 13 pointers used to tune the $\delta^{18}O$ data of core MD99-2339 to the NGRIP chronology, by considering GI onsets (numbers 1 to 12 on the Figure) according to Wolff et al. (2010). Sedimentation rates, calculated between different pointers of core MD99-2339, are also highlighted with the dark histogram. YD: Younger Dryas, BA: Bölling-Alleröd. b) A zoom on the interval 25 - 50 ka BP enables to better consider the pointers selected (dotted vertical lines) for this new age model.

**Figure 4:** Data from core MD99-2339 against depth (cm). $\delta^{18}O$ planktonic monospecific record of core MD99-2339 (a, Voelker et al., 2006), is presented in parallel with the W/C qualitative index of surface temperatures (b). Diversity indexes (species richness according to the Margalef index, c, and dominance, d) are drawn in parallel with percentages of the major species *L. machaerophorum* (e). Different calculations of dinocyst concentrations (f, g) are represented in linear scale, while h) illustrates total dinocyst and *L. machaerophorum* concentrations in logarithmic scale, compared with sedimentation rates (i) and dinocyst fluxes (j). GI: Greenland Interstadial. Grey bands indicate Heinrich Stadials (HS) and the Younger Dryas (YD).

**Figure 5:** Data from core MD99-2339 against age (cal ka BP): major taxa occurring with values higher than 2% in dinocyst assemblages from MD99-2339 core (0 - 48 ka BP; 0 - 1,854 cm). Red, blue and green colours respectively indicate the "Warm", "Cold", and "Heterotrophic" groups. W/C: Warm-Cold Ratio. The trends shown in grey are calculated by excluding *Lingulodinium machaerophorum* from the main dinocyst sum, while coloured curves (colours explained in the Figure) depict the whole assemblage considering all species. MD04-2805 CQ dinocyst data are also represented over the 28 ky BP so as to illustrate similarities between the assemblages from the central (MD99-2339, this study) and southern (MD04-2805 CQ; Penaud et

al., 2011a) Gulf of Cadiz. Pink bands indicate warmer intervals (including BA: Bölling-Alleröd, LGM: Last Glacial Maximum, GI: Greenland Interstadial) and blue bands indicate colder events (HS: Heinrich Stadials and YD: Younger Dryas).

**Figure 6:** Data from core MD99-2339 against age (cal ka BP). $\delta^{18}O$ planktonic monospecific record and *N. pachyderma* s. percentages from core MD99-2339 (Voelker et al., 2006) in parallel with dinocyst transfer function results (n= 1492; Radi and de Vernal, 2008) : Winter and Summer Sea Surface Temperature (SST) and Sea Surface Salinity (SSS), as well as Seasonality (SST summer - SST Winter) and Annual Productivities. Total dinocyst and heterotrophic fluxes are also depicted with the ratio H/A for "Heterotrophics / Autotrophics", and percentages of two species: *L. machaerophorum* as a species index for higher surface stratification linked with increased paleo-river discharges and *B. tepikiense* as a species index for thermal seasonal contrasts. Stars on each graph indicate present-day values for dinocyst percentages and hydrological parameters recorded in modern sediments and overlying surface waters, respectively, at the coordinates of analogue "A184" in the modern dinocyst database (34.32°N, 7.02°W; http://www.geotop.ca/fr/bases-de-donnees/dinokystes.html) : SST Winter of 16.48°C and SST Summer of 22.47°C, SSS Winter of 36.35 and SSS Summer of 36.33, Mean Annual Productivity of 85.7 $gC.m^{-2}$, percentages of *L. machaerophorum* of 65.27% and *B. tepikiense* of 0%.

**Figure 7:** Greenland $\delta^{18}O$ data (a) in parallel with data from core MD99-2339: planktonic $\delta^{18}O$ (b) and mean grain-size <63 µm (c), over the last 50 ky. Dinocyst data (f, h, i, j) from core MD99-2339 are also depicted *versus* Western (pollen, Alboran Sea, g) and Eastern ($\delta^{18}O$, Soreq Cave, m) Mediterranean records, as well as orbital parameters (d, e). Sedimentation rates (l) calculated from the new age model of core MD99-2339 echoe total dinocyst concentrations (k). Greenland Interstadials (GI) 1 (Bölling-Alleröd: BA), 8 and 12 are highlighted with yellow bands and are characterized by a bipartite structure labelled "a" and "b" for the first and second phases, respectively. Grey bands indicate Heinrich Stadials (HS) and the Younger Dryas (YD). Orange vertical band indicates the time interval corresponding to sapropel 1 (S1) formation (9.5 - 6.5 ka BP).

**Figure 8:** Comparison between dinocyst data (percentages or concentrations) as recorded from each side of the Strait of Gibraltar. Full blue / blue curves represent MD99-2339 data (Gulf of Cadiz, this study) while full red / red curves represent MD95-2043 data (Alboran Sea, Penaud et al., 2011b). Greenland Interstadials (GI) 8 and 12 are highlighted with yellow bands and are characterized by a bipartite structure labelled "a" and "b" for the first and second phases, respectively. Other GIs are highlighted with pink bands also corresponding to the numbered peaks obvious on the NGRIP curve. Grey bands indicate Heinrich Stadials (HS).

1339 See Supplement Material for Table 1

1340

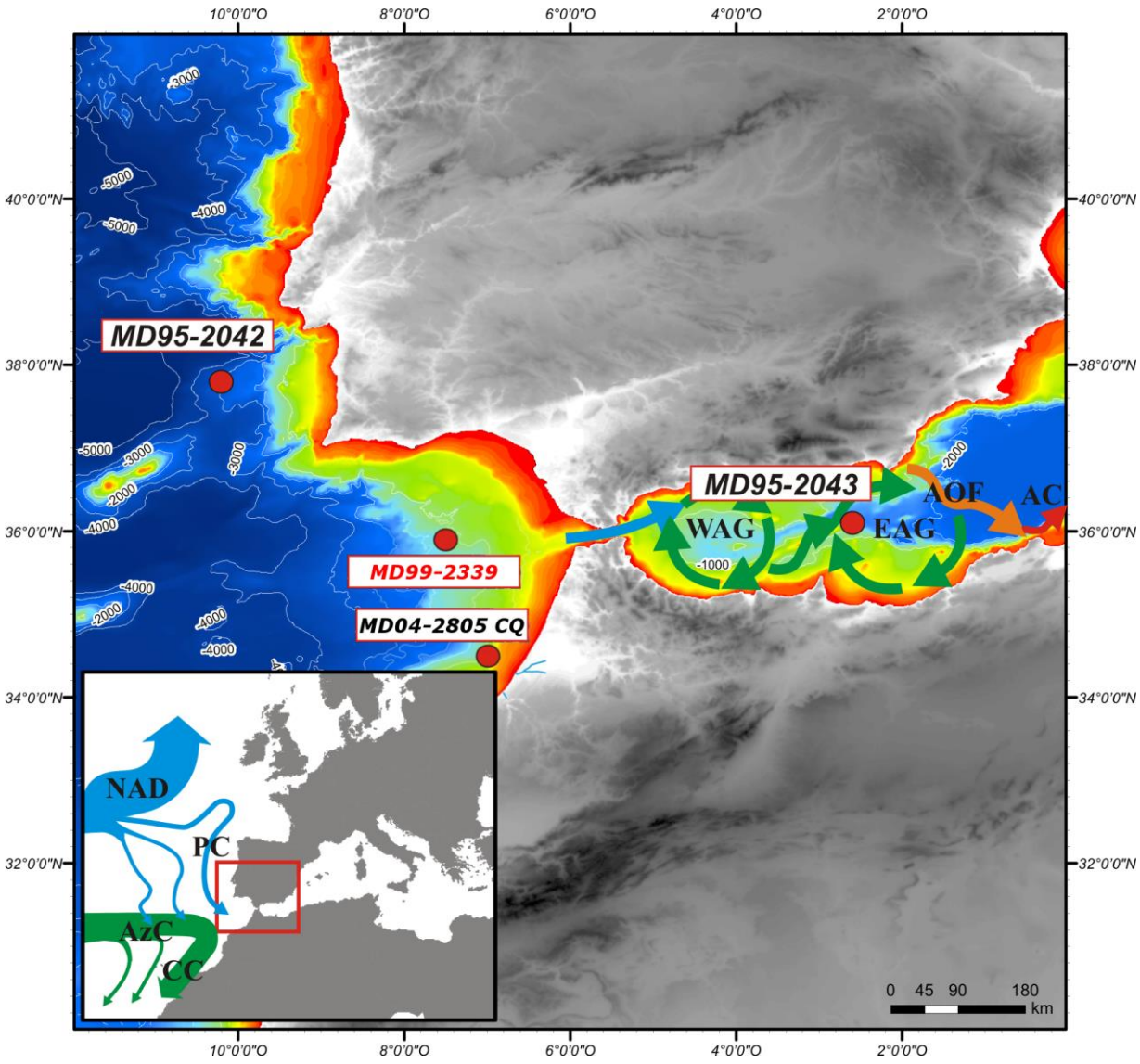


1341

1342

1343 Figure 1

1344

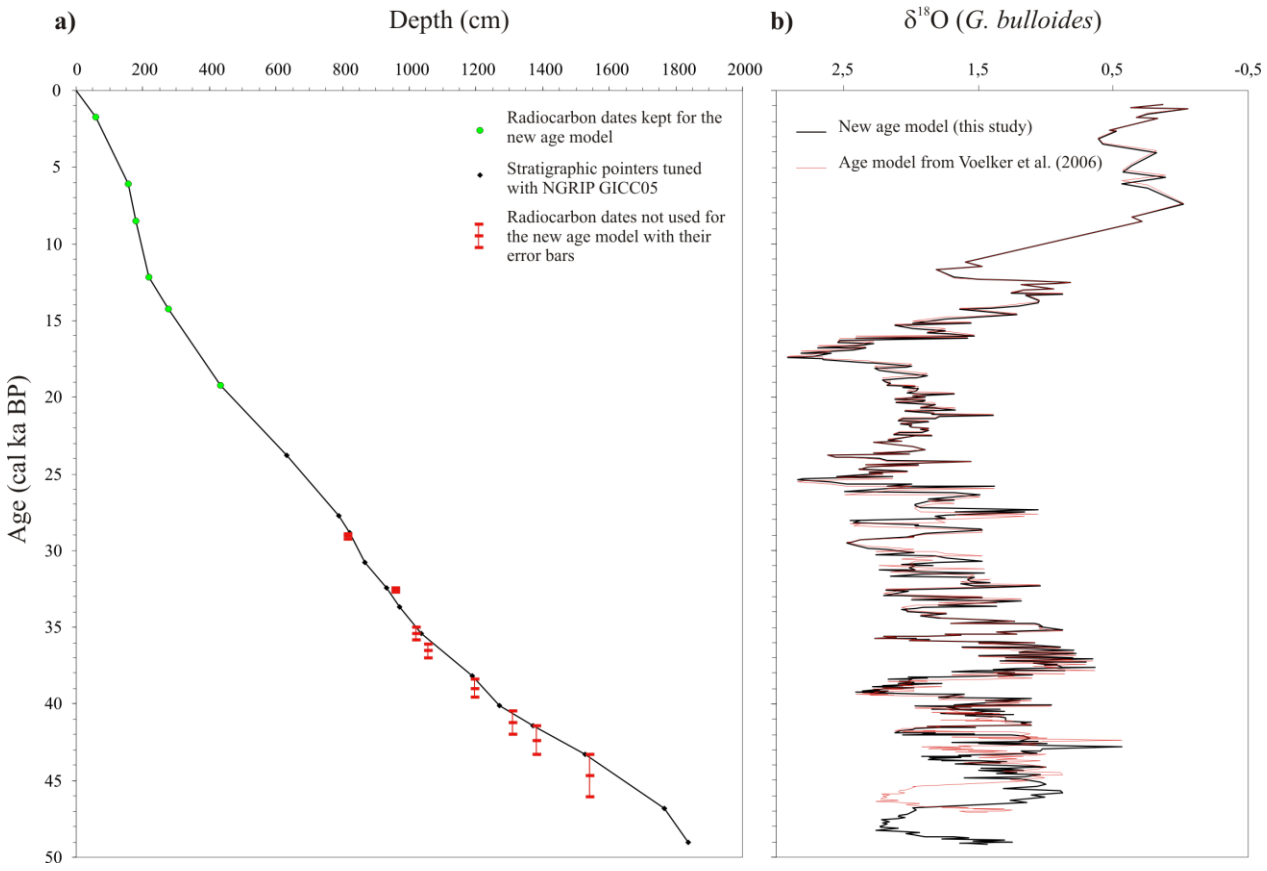


1345

1346 Figure 2

1347

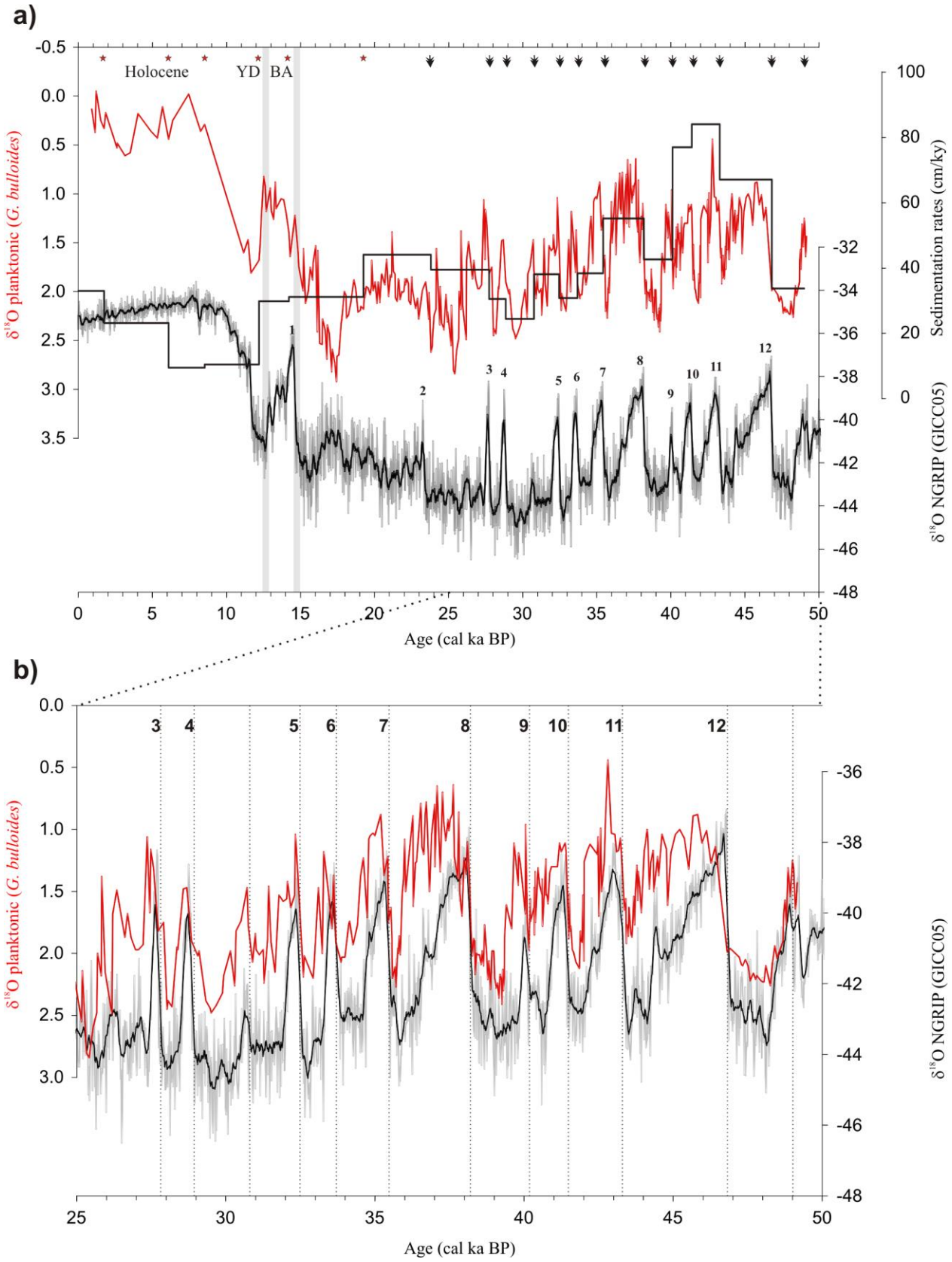


1348

1349

1350 Figure 3

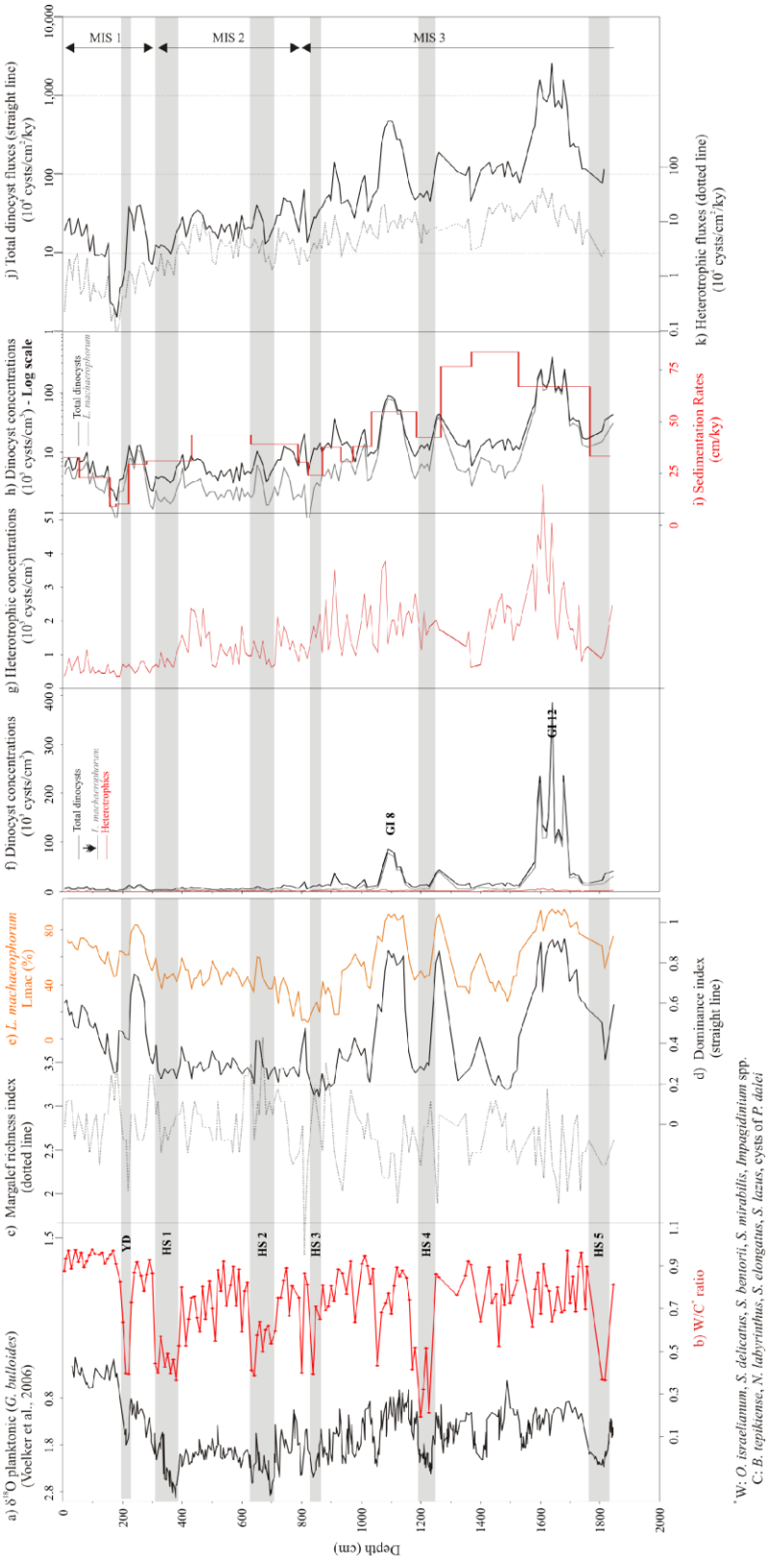
MIS 1
MIS 2
MIS 3
j) Total dinocyst fluxes (straight line) (10³ cysts/cm²/ky)
k) Heterotrophic fluxes (dotted line) (10³ cysts/cm²/ky)
h) Dinocyst concentrations (10³ cysts/cm³) - Log scale
Total dinocysts
L. machaerophorum
i) Sedimentation Rates (cm/ky)
g) Heterotrophic concentrations (10³ cysts/cm³)
f) Dinocyst concentrations (10³ cysts/cm³)
Total dinocysts
L. machaerophorum
Heterocephalus
GI 8
GI 12
e) L. machaerophorum Linac (%)
e) Margalef richness index (dotted line)
d) Dominance index (straight line)
a) δ¹⁸O planktonic (G. bulloides) (Voelker et al., 2006)
b) W/C* ratio
YD
HS 1
HS 2
HS 3
HS 4
HS 5
Depth (cm)
*W: O. israeliannm, S. delicatus, S. hemorii, S. mirabilis, Impagidinium spp.
C: B. tepikiense, N. labyrinthus, S. elongatus, S. lazus, cysts of P. dalei

Figure 4

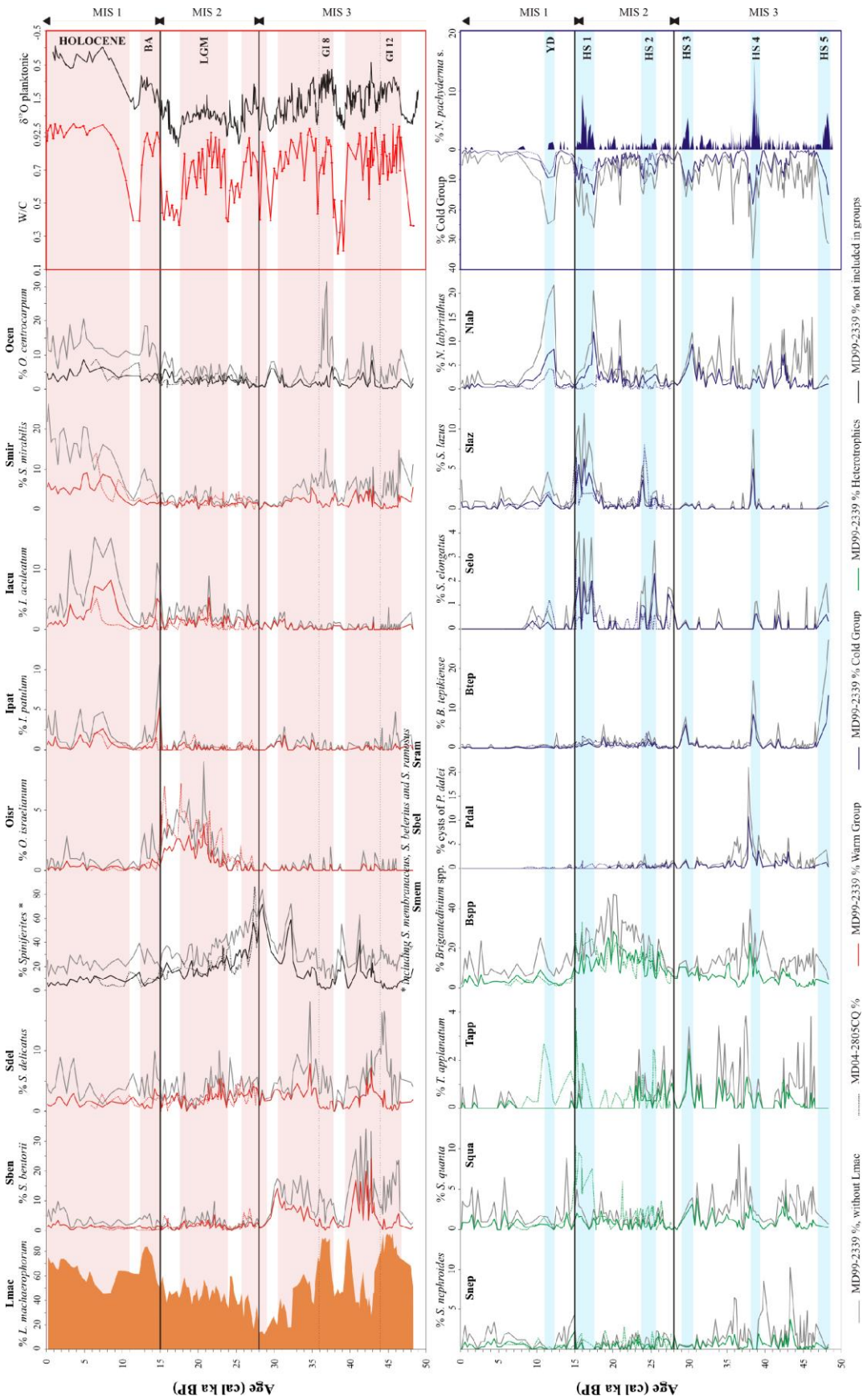
MIS 1
MIS 2
MIS 3
HOLOCENE
BA
LGM
GI 8
GI 12
YD
HS 1
HS 2
HS 3
HS 4
HS 5
δ18O planktonic
W/C
% N. pachyderma s.
% Cold Group
Ocen
% O. centrocarpum
Nlab
% N. labyrinthus
Smir
% S. mirabilis
Slaz
% S. lazus
Iacu
% I. aculeatum
Selo
% S. elongatus
Ipat
% I. patulum
Btep
% B. tepikiense
Sram
Sbel
Oisr
% O. israelianum
% cysts of P. dalei
Pdal
Smem
% Spiniferites *
Bspp
% Brigantedinium spp.
* including S. membranaceus, S. belerius and S. ramosus
Sdel
% S. delicatus
Tapp
% T. applanatum
Sben
% S. bentorii
Squa
% S. quanta
Lmac
% L. machaerophorum
Snep
% S. nephroides
Age (cal ka BP)
MD99-2339 %, without Lmac
MD04-2805CQ %
MD99-2339 % Warm Group
MD99-2339 % Cold Group
MD99-2339 % Heterotrophics
MD99-2339 % not included in groups

Figure 5

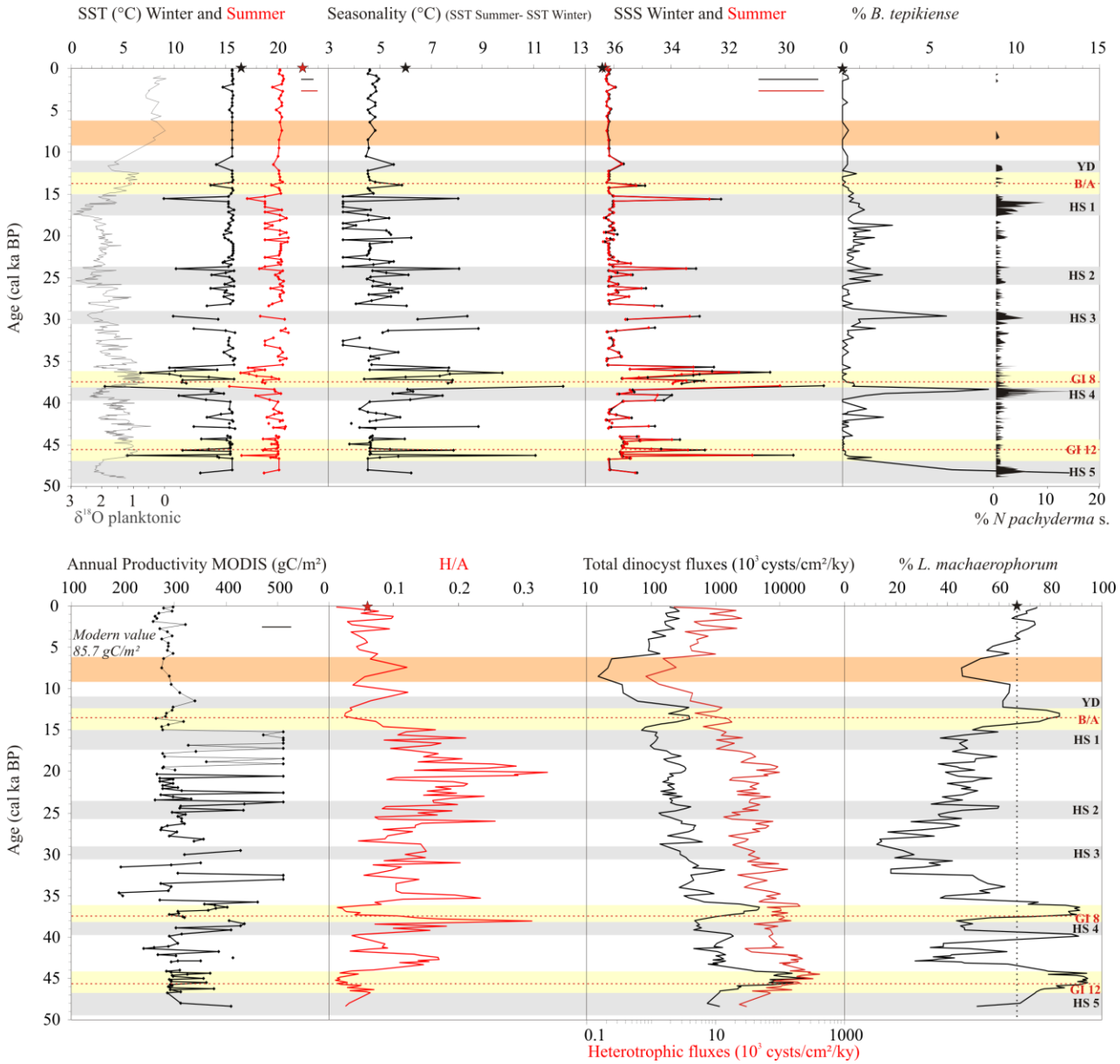


1401

1402 Figure 6

1403

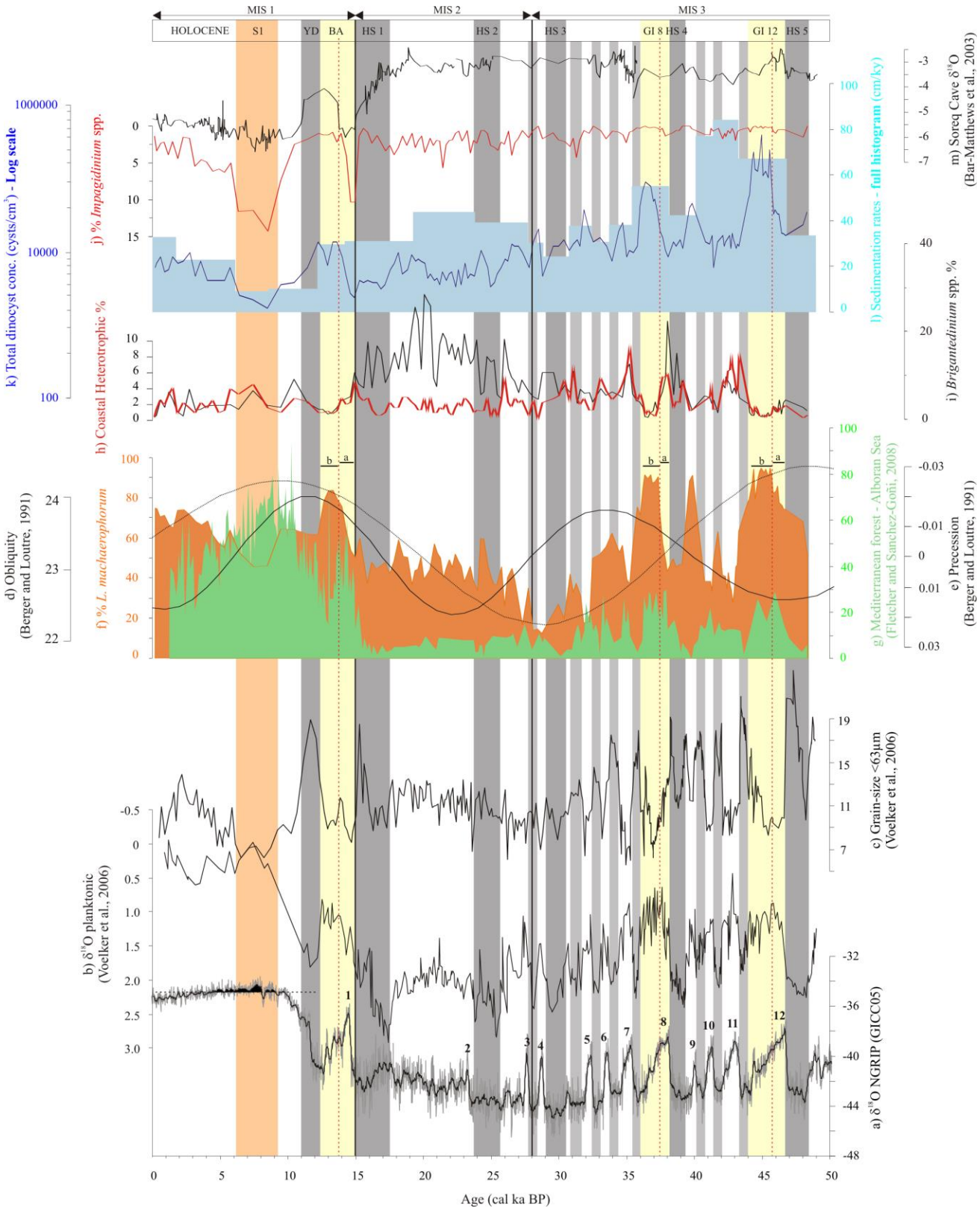


1404

1405

1406 Figure 7

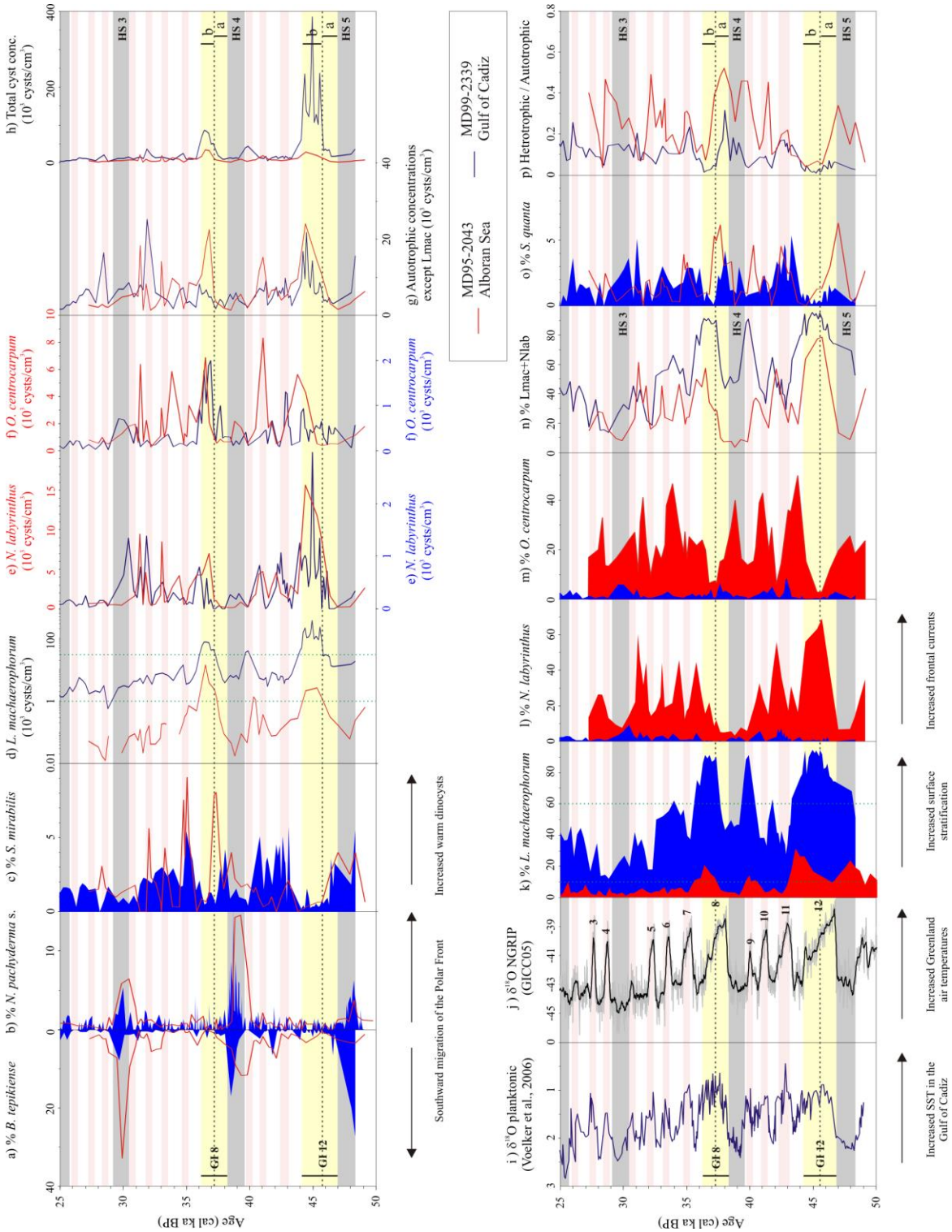
MD95-2043
Alboran Sea
MD99-2339
Gulf of Cadiz
HS 3
HS 4
HS 5
GI 8
GI 12
Age (cal ka BP)
Southward migration of the Polar Front
Increased warm dinocysts
Increased surface stratification
Increased frontal currents
Increased Greenland air temperatures
Increased SST in the Gulf of Cadiz

Figure 8